FGFR2 ACTIVATION MEDIATES NANOG REPRESSION DURING PRIMITIVE ENDODERM DIFFERENTIATION IN MURINE EMBRYONIC STEM CELLS

By

KATHERINE ELIZABETH HANKOWSKI

A DISSERTATION PRESENTED TO THE GRADUATE SCHOOL
OF THE UNIVERSITY OF FLORIDA IN PARTIAL FULFILLMENT
OF THE REQUIREMENTS FOR THE DEGREE OF
DOCTOR OF PHILOSOPHY

UNIVERSITY OF FLORIDA

2011

To my family for their love and support

ACKNOWLEDGMENTS

I would like to first thank my mentor, Dr. Naohiro Terada, for welcoming me into his lab and supporting me throughout my graduate studies. Without Dr. Terada's patience, motivation, and guidance none of this work would have been possible. I would also like to thank all of my committee members, Dr. Jörg Bungert, Dr. Paul Oh, Dr. Peter Sayeski, and Dr. Stephen Sugrue, for their insightful comments, suggestions, and for generously sharing their expertise and individual points of view.

Next, I would also like to thank past and present members of Dr. Terada's lab. In particular, Dr. Takashi Hamazaki, who taught me much about stem cell biology and was always willing to listen and help, and Dr. Amar Singh for opening my eyes to the wonder of stem cells by showing me beating cardiomyocytes when I came to the lab in my first laboratory rotation. I would also like to thank Dr. Jeffrey Brower, Dr. Sarah Kehoe, Dr. Aline Bonilla, Chae Ho Lim, Milena Leseva, and Amy Meacham for their support and friendship.

Finally, I would like to thank my wonderful family and friends, especially my parents, brother, and sister for supporting me through twenty-six years of school; my friend Mimosa McNerney, my fiancé Charlie Santostefano, and Ann and Vince Santostefano for their kindness and support; without them I would certainly have missed out on much that Florida has to offer.

TABLE OF CONTENTS

page

LIST OF TABLES

LIST OF FIGURES

LIST OF ABBREVIATIONS

E3.5	Embryonic day 3.5 early blastocyst stage embryo
E4.5	Embryonic day 4.5 late blastocyst stage embryo
α	Alpha
AFP	Alpha-fetoprotein
β	Beta
β–geo	betagalactosidase- neomycin fusion gene
BMP4	Bone morphogenic protein 4
BP	Base pair
°C	Degrees Celsius
cDNA	Complementary DNA
ChIP	Chromatin immunoprecipitation
CO_2	Carbon dioxide
DNA	Deoxyribonucleic acid
EBs	Embryoid bodies
ES cells	Embryonic stem cells
EPI	Epiblast
FBS	Fetal bovine serum
FGF	Fibroblast growth factor
FGFR2	Fibroblast growth factor receptor 2
Frs2	Fibroblast growth factor receptor substrate 2
GFP	Green fluorescence protein
Grb2	Growth factor receptor-bound protein 2
H3K4me3	Histone 3 lysine 4 trimethylation
H3K9me3	Histone 3 lysine 9 trimethylation

H3K27me3	Histone 3 lysine 27 trimethylation
H3K36me3	Histone 3 lysine 36 trimethylation
ICM	Inner cell mass
Id	Inhibitor of differentiation
JAK	Janus associated kinase
LIF	Leukemia inhibitory factor
MAPK	Mitogen-activated protein kinase
mg	Milligram
μg	Microgram
mL	Milliliter
μl	Microliter
mM	Millimolar
ng	Nanogram
nM	Nanomolar
PBS	Phosphate buffered solution
PCR	Polymerase chain reaction
PE	Primitive endoderm
PI3K	Phosphatidylinositol 3-kinase
PLCγ	Phosphoinositide phospholipase C gamma
RNA	Ribonucleic acid
RNA Pol II	RNA polymerase II
RPM	Revolutions per minute
Shp2	Src homology region 2 domain-containing phosphatase 2
Sos	Son of sevenless homology
TE	Trophectoderm

Abstract of Dissertation Presented to the Graduate School
of the University of Florida in Partial Fulfillment of the
Requirements for the Degree of Doctor of Philosophy

FGFR2 ACTIVATION MEDIATES NANOG REPRESSION DURING PRIMITIVE ENDODERM DIFFERENTIATION IN MURINE EMBRYONIC STEM CELLS

By

Katherine E. Hankowski

May 2011

Chair: Naohiro Terada
Major: Medical Sciences- Molecular Cell Biology

Pluripotency of murine embryonic stem (ES) cells is maintained by the precise coordination of signaling cascades and transcriptional networks promoting proliferation and preventing differentiation. During mouse preimplantation development, pluripotent stem cells give rise to the primitive endoderm (PE) layer on the surface of the inner cell mass (ICM). This first differentiation step occurs through the loss of Nanog expression in these cells, and is accompanied by an increase in the expression of Gata6. Nanog expression is essential for self-renewal both in vivo in the ICM of the blastocyst and in vitro during ES cell culture. Our lab has identified the importance of fibroblast growth factor receptor 2 (FGFR2) and the downstream Ras/Mek/Erk signaling pathway in *Nanog* repression and subsequent differentiation to PE. Using an inducible FGFR2 dimerization system, we demonstrate that FGFR2 downregulated *Nanog* gene transcription rapidly and selectively among pluripotency regulatory genes. This downregulation of *Nanog* was accompanied by accumulation of RNA Polymerase II at the transcription start site and occurred without an increase in repressive histone methylation marks, implying regulation is likely in the early phase of gene repression and/or is reversible. Moreover, the proximal promoter region of *Nanog* containing the

minimum Oct4/Sox2 binding site was sufficient for *Nanog* transcriptional downregulation by FGFR2 using insulated and integrated reporter constructs. Interestingly, using chromatin immunoprecipitation, we found Oct4 and Sox2 transcription factors, which are essential for positive *Nanog* transcription, remain bound to the proximal promoter region. The importance of this region containing Oct4/Sox2 binding sites and the persistence of Oct4 and Sox2 transcription factors binding following *Nanog* downregulation suggests these factors may interact with different proteins to mediate both *Nanog* transcriptional activation and repression. These findings provide insight into fluctuations seen in Nanog in ES cell culture and lend support to the idea that cells derived from the ICM are plastic, their expression of Nanog and Gata6 change, and they are able to develop into PE and epiblast. In addition, understanding the mechanism for *Nanog* repression will increase our knowledge of how extrinsic differentiation factors are linked to the intrinsic network that controls cell-fate specification.

CHAPTER 1
INTRODUCTION

Murine Preimplantation Embryonic Development

Following fertilization of the oocyte by sperm, the early mouse embryo undergoes three cleavage divisions to increase from the 1-cell to 8-cell stage. During these cleavage divisions, the cells known as blastomeres undergo mitosis and produce progressively smaller daughter cells to maintain the overall size of the embryo [1, 2]. The blastomeres of the 8-cell embryo increase their intercellular contacts and adopt a flattened morphology, developing into a compacted morula.

During compaction, adherens junctions form as E-cadherin localizes to cell-cell contacts, gap junctions form between blastomeres, and the blastomeres polarize along the axis of cell contact, to form outer facing apical regions and inner facing basolateral regions with tight junctions[2-4]. As the embryo further develops to the 16-cell and 32-cell late morula stage embryo, blastomeres undergo symmetric or asymmetric cell division depending on orientation of the cleavage plane[2]. Blastomeres that undergo mitosis parallel to the inside-outside axis divide symmetrically to produce two polar cells that remain on the outside of the embryo, while blastomeres that divide perpendicular to the inside-outside axis produce two asymmetrical cells, one polar outer cell and one apolar cell that is located inside the embryo[2, 3]. As the outside cells of the embryo become committed to the trophectoderm (TE) epithelial layer, the fluid filled blastocoel cavity begins to form in the 32-cell late morula stage embryo.

Blastocoel fluid is mainly composed of water, and enters the embryo through the TE epithelium. Na^+/K^+ ATPase located in the basolateral region of TE cells is thought to create a trans-trophectoderm Na^+ gradient by actively transporting Na^+ out of the TE cell

into the embryo[2, 4]. This is proposed to drive the movement of water by osmosis and possibly through aquaporins across the TE epithelium into the extracellular space of the embryo to form the fluid-filled blastocoel[2, 4]. This fluid-filled cavity is maintained by the TE tight junctions, which allow for expansion of the blastocoel, and the collection of pluripotent cells known as the inner cell mass (ICM) is pushed to one end of the embryo. The embryo is now considered to be an early blastocyst, and contains specified TE and ICM lineages.

Lineage Specification to Trophectoderm and Inner Cell Mass

TE and ICM are the first lineages specified in the preimplantation embryo. Based upon experimental observations, early investigators proposed two different models for how lineage specification occurs: the inside-outside model[5] and the cell polarity model[6]. According to the inside-outside model, cell fate is specified in the 16-cell morula stage by cell position in the embryo. They proposed that differences in cell-cell contacts and surrounding microenvironments between inner and outer cells dictate that outer cells become specified to the TE lineage while inner cells become part of the ICM [2, 7]. Later, investigators proposed the cell-polarity model of lineage specification when they discovered blastomeres polarize and asymmetrically divide to form polar and apolar cells[2]. According to this model, at the 8-cell stage, cell fate depends on inheritance of polarity during cell divisions. Cells which undergo symmetrical division produce two polar outer cells which will become TE cells in the blastocyst. Cells which divide asymmetrically will produce one outer polar cell specified to the TE lineage, and one inner apolar cell specified to the ICM lineage [2, 7]. Currently, there is evidence to support lineage specification to TE and ICM based on both cell polarity and cell position, and likely both contribute to cell fate specification.

Transcription factor expression plays a critical role in specification to TE and ICM lineages. The caudal type homeobox 2 (Cdx2) transcription factor is first expressed at low levels in the 8-cell stage embryo[8]. Its expression increases in outer cells of the 16-cell embryo while decreasing in inner cells and this expression pattern becomes more pronounced by the 32-cell embryo, where Cdx2 is highly expressed in outer cells that will become TE in the blastocyst[8]. The POU domain transcription factor Oct4 is weakly expressed in oocytes and early cleavage stage embryos and becomes highly expressed in nuclei of the 8-cell embryo and in all cells of the morula[9, 10]. Soon after, expression is restricted to the ICM of the blastocyst, and Oct4 expression is lost in the outer, trophectoderm layer[9, 10].

Cdx2 expression becomes restricted earlier than Oct4 and another important transcription factor, Nanog. It is thought that Cdx2 may downregulate expression of these genes in the outer TE layer[2]. This is supported by *Cdx2* null embryos which improperly express Oct4 and Nanog in the outer TE-like layer in blastocyst stage embryos in contrast to wild type embryos where Oct4 and Nanog expression is restricted to the ICM[11]. These null embryos initially form a blastocoel cavity, but it cannot be maintained, and they die around the time of implantation[11] Oct4 is required for formation of the ICM as null embryos develop to the blastocyst stage but lack pluripotent ICM cells and are composed of trophectoderm cells[12]. These embryos die prior to egg cylinder formation[12].

Lineage Commitment to Primitive Endoderm and Epiblast

During maturation from the early to late blastocyst stage embryo, the ICM surface gives rise to a monolayer of cells facing the blastocoel cavity known as the primitive endoderm (PE) layer[2]. PE later develops into two extraembryonic cell types, parietal

and visceral endoderm. Parietal endoderm is a single layer of cells which develops along with the trophectoderm. It synthesizes large amounts of extracellular matrix proteins type IV collagen and laminins which assemble to form Reichert's membrane, a specialized basement membrane that surrounds the developing embryo and passively filters nutrients[13]. Visceral endoderm cells develop along with the epiblast. These cells have microvilli and contain numerous phagocytic and pinocytic vesicles to allow for efficient absorption and digestion of maternal nutrients[13]. In addition, visceral endoderm cells also synthesize and secrete proteins which are involved in nutrient transport[13].

At the last blastocyst stage, the ICM of pluripotent cells is known as the epiblast (EPI), which goes on to form the embryo proper. The transcription factor Nanog is critical for cell fate specification to the EPI. This homeodomain transcription factor is expressed in the morula stage embryo, ICM of the blastocyst, EPI, and is later downregulated as EPI cells enter the primitive streak[14]. Nanog is required for maintenance of ICM pluripotency and formation of the EPI, as null embryos form a normal ICM in the early blastocyst stage, but late blastocyst stage embryos lack EPI and form only PE[15].

Early models for understanding PE or EPI specification were similar to the inside-outside model of TE specification, where cell position dictated lineage commitment. In this model, the ICM is a homogeneous collection of cells that are able to form either lineage, and that cells on the surface of the ICM would develop into the PE, while those on the inside would become EPI[2]. More recent data has shown the position of a cell in the ICM does not always correlate with its cell fate.

While Oct4 is expressed at comparable levels in all cells of the ICM of the early blastocyst stage embryo, Nanog is heterogeneously expressed, where some cells express high levels while other express low levels[15]. Surprisingly, the primitive endoderm marker Gata6 is also heterogeneously expressed in the ICM, in a mutually exclusive manner to Nanog expression, which results in cell that express either Nanog or Gata6[16]. In addition, Nanog+ and Gata6+ cells are not spatially organized, but rather randomly distributed in a so-called "salt and pepper" pattern[16]. Additionally, growth factor receptor-bound protein 2 (Grb2) null E3.5 embryo ICM cells express high levels of *Nanog* mRNA and protein rather uniformly, while Gata6 expression is absent. This indicates Grb2 and downstream mitogen-activated protein kinase (MAPK) signaling plays an important role in lineage segregation to PE. This salt and pepper pattern is sorted out by the E4.5 late blastocyst stage to form an outer Gata6+ PE layer and an inner Nanog+ EPI population[15]. Using this evidence, an alternative model of PE and EPI specification is proposed where an individual cell's sensitivity to MAPK signaling dictates whether it will become PE or EPI[15].

Fibroblast Growth Factor Receptor Signaling is Essential for Primitive Endoderm Differentiation

Fibroblast growth factor (FGF) ligands, their receptors, and downstream signaling cascades control many important processes during mammalian development including proliferation, migration, and differentiation[17, 18]. FGFs are secreted molecules which activate specific tyrosine kinase receptors known as fibroblast growth factor receptors (FGFRs). FGFRs are present as inactive monomers in the plasma membrane and activation occurs when FGF molecules connected by a heparin sulfate proteoglycan bind to the extracellular domains of the receptor and cause homodimerization[17]. This

leads to autophosphorylation of tyrosine residues in the intracellular region of the receptor[17]. These receptors activate various pathways including the phosphoinositide phospholipase C gamma (PLCγ), phosphatidylinositol 3-kinase (PI3K), and the MAPK signaling cascades[17].

In MAPK Mek/Erk signaling, fibroblast growth factor receptor substrate 2 (Frs2), a membrane anchored docking protein, is phosphorylated at tyrosine residues, which allows for binding of the small adaptor molecule growth factor receptor-bound protein 2 (Grb2), and Src homology region 2 domain-containing phosphatase 2 (Shp2)[17]. Grb2 exists in a complex with son of sevenless homology (Sos), the nucleotide exchange factor, which catalyzes the exchange of GDP for GTP on Ras, the GTP binding protein[17]. Ras activates downstream factor Raf, which activate Mek1 and Mek2 by phosphorylation of two serine residues at amino acids 217 and 221. Mek1 and Mek2 activate Erk1 (p44) and Erk2 (p42) by phosphorylation of amino acids Thr202/Tyr204 and Thr185/Tyr187, respectively, and Erk1/2 subsequently enters the nucleus where it phosphorylates target transcription factors.

Among the 22 FGF ligands and 5 receptors, Fgf4 and FGFR2 are critical during mouse early embryonic development as null mutations in these are lethal around the time of implantation[19]. Fgf4 is the most highly expressed FGF ligand in the pre-implantation embryo, where it is detectable in the 8-cell morula and later becomes restricted to the EPI of the late blastocyst stage embryo[19]. FGFR2 is also the major receptor expressed in the blastocyst embryo, though FGFR1 is also found[19]. FGFR1 is thought to function later in the embryo as null embryos display post-implantation abnormalities[19].

Disruption of FGFR2 prevents PE formation[20], and when FGF signaling is blocked by overexpression of a dominant negative mutant of FGFR2 or by the FGFR specific inhibitor SU5042, primitive endoderm layer formation is eliminated [21-23]. These data strongly support the importance of FGF-FGFR interaction and signaling is critical for PE differentiation. In addition, disruption of Grb2 prevented the formation of PE in blastocysts, a phenotype that can be rescued by expression of a Grb2-Sos fusion protein[24]. Introduction of an active Ras mutant in ES cells resulted in PE differentiation[25]. Together, these studies suggest the Ras/Mek/Erk pathway plays a vital role in PE specification.

Murine Embryonic Stem Cells

In 1981, embryonic stem (ES) cells were first derived from cells of the ICM of the blastocyst [26, 27]. These cells have an unlimited capacity to self-renew and are deemed pluripotent due to their ability to differentiate into ectoderm, endoderm, and mesoderm [28, 29]. Morphologically, ES cells grow as smooth dome-shaped colonies when maintained during *in vitro* cell culture.

Extrinsic and Intrinsic Factors Maintain Embryonic Stem Cell Self-renewal

At the beginning, ES cells were maintained on a layer of mitotically inactivated mouse embryonic fibroblasts (MEFs) in cell culture media supplemented with fetal bovine serum (FBS). The feeder layer provided a substrate for ES cell attachment and secreted factors to maintain pluripotency and prevent differentiation. The cytokine leukemia inhibitory factor (LIF) was later identified as the essential factor secreted from fibroblasts which can maintain ES cells in an undifferentiated state[30, 31]. This discovery revolutionized ES cell culture and made it possible to maintain ES cells on gelatin-coated dishes by supplementing cell culture media with purified LIF. When LIF is

withdrawn from the media, ES cells quickly differentiate into endoderm, ectoderm, and mesoderm lineages [28-30].

LIF is a member of the Interleukin-6 (IL-6) cytokine family. LIF binds to the heterodimeric receptor LIF receptor (LIFR) and gp130, which leads to activation of Janus associated kinase (JAK) and signal transducer and activator of transcription3 (STAT3). STAT3 activation by tyrosine phosphorylation induces STAT3 dimerization and translocation to the nucleus where it regulates genes involved in maintaining self-renewal, including the transcription factor c-Myc[32, 33]. LIF alone in serum-free conditions is insufficient to maintain ES cell self-renewal and leads to neural differentiation[34]. This indicated another factor must cooperate with LIF to maintain self-renewal and prevent neural differentiation. FBS, which was added to the cell culture media, contained many unknown factors which helped maintain ES cell. One of such factors, bone morphogenic protein 4 (BMP4) was shown to support self renew when added in conjunction with LIF[35].

BMP4 is one of over twenty BMPs which are involved in the regulation of important cellular processes including proliferation, differentiation, and apoptosis[35]. BMPs bind to their receptors to cause dimerization and activation of Smad proteins 1, 5, and 8 by phosphorylation, which induces their translocation to the nucleus where they influence expression of inhibitor of differentiation (Id) genes to block neural differentiation[36, 37]. Constitutive expression of Id1, Id2, or Id3 is able to bypass the requirement of BMP, and over-expression of Ids is able to compensate for the removal of BMP from ES cell culture, but not LIF[38]. Both the LIF/STAT and BMP/Smad pathways work together to maintain ES cell self-renewal (Figure 1-1).

In addition to extrinsic factors like LIF and BMP4, intrinsic factors have been found to be critical for ES cell maintenance. These include the master transcriptional regulators Nanog, Oct4, and the SRY-related HMG domain family member Sox2. These transcription factors are shown to bind together to their own promoters and there is evidence they form an autoregulatory loop to maintain their expression[39]. In addition, Oct4 and Sox2 have been shown to form a complex and bind cooperatively to control gene expression of *Fgf4*, *Utf1*, *Fbx15*, *Lefty1*, *Oct4*, *Sox2*, and *Nanog*[40-47]. Interestingly, Oct4, Sox2, and Nanog bind together to hundreds of genes, some active genes that promote ES cell self-renewal and some inactive genes that promote differentiation[48]. Currently, however, it is not well understood what other factors assist Oct4, Sox2, and Nanog in mediating gene activation or repression and how these factors change as ES cells differentiate.

ES cells are not a homogeneous population of cells, but are rather heterogeneous in the expression of several genes including pluripotency associated genes: platelet/endothelial cell adhesion molecule (Pecam1), Rex1, Stella, stage specific antigen1 (SSEA1)[19]. In addition, a subset of ES cells has been shown to express genes associated differentiation including brachyury, Hex, and Sox17[19]. We have demonstrated that Nanog and Gata6 are also heterogeneously expressed in ES cells[60]. Indeed, ES cells can be divided into two populations: Nanog-high cells and Nanog-low cells, which express the PE marker Gata6, indicating ES cells closely resemble the ICM cells they are derived from[60]. This indicates that ES cells serve as a good model system for understanding early embryonic development. When cells are sorted into Nanog+ and Nanog- cells and grown in vitro, they can regenerate the initial

heterogeneity, indicating these cells retain plasticity[60]. If Nanog+ and Nanog- cells are induced to differentiate using LIF removal from the cell culture media, Nanog low cells show increased expression of the primitive endoderm markers Gata4 and Gata6, indicating these cells are committed to PE differentiation[60]. In addition, we have shown that Nanog directly controls Gata6 expression by binding to its promoter region to repress the gene[60]. Overexpression of Nanog is able to reduce heterogeneity during ES cell maintenance.

Promoting Embryonic Stem Cell Differentiation to Primitive Endoderm

ES cell differentiation can be achieved in a variety of ways. One method is by aggregating cells in suspension culture to form embryoid bodies (EBs)[49]. These recapitulate many aspects of early embryonic development and differentiate into cells of all three embryonic germ layers. EBs are classically formed by the "hanging drop" method. In this method, ES cells are dissociated into a suspension of single cells and equal numbers of ES cells are suspended in media suspended from the lid of a Petri-dish. After two days, the ES cells form round EB aggregates that are uniform in size. These can then be collected and resuspended in fresh media for an additional few days to increase in size. After four days, EBs are collected and attach to cell culture dishes where they differentiate further and form outgrowths.

PE differentiation can be observed during the differentiation of ES cells using the hanging drop technique. PE cells cluster in the outer periphery of EBs after 2 days of differentiation[50]. We previously found that EBs formed in the presence of LIF and serum (in ES cell maintenance media) are able to produce an outer layer that has differentiated to PE, which we visualized by aggregating ES cells that express green fluorescence protein (GFP) driven by the α-fetoprotein (AFP-GFP) promoter[50]. In these

EBs, GFP was clearly visible after 2 days in the outer layer in the presence of LIF[50]. Using fluorescent-assisted cell sorting (FACS) to isolate GFP positive and negative populations, subsequent examination of mRNA expression patterns showed that the negative population expressed pluripotency related genes while the positive population expressed markers of primitive endoderm[50]. Additionally, ES cells that express β-galactosidase under the control of the endogenous *Nanog* promoter do not stain for X-gal in the outer PE layer when aggregated in media containing LIF[50]. This suggests aggregation leads to the downregulation of *Nanog* in the outer PE layer.

To determine if *Nanog* overexpression can inhibit PE differentiation, an inducible Nanog overexpression system was used where Nanog is under the control of the tetracycline inducible system (Tet-off). Upon aggregation of ES cells in LIF containing media by the hanging drop method, PE positive cells developed in the outer layer in the presence of doxycycline, as expected, but not in the absence, when Nanog is overexpressed[50]. This data suggests that Nanog overexpression prevents differentiation to PE. The mechanism for Nanog downregulation during PE differentiation in the outer layer of ES cell aggregates has been connected to the FGFR/Ras/Mek/Erk signaling pathway.

We have shown that increasing protein tyrosine phosphorylation using sodium vanadate, a protein tyrosine phosphatase inhibitor, represses *Nanog* and leads to PE differentiation[51]. Remarkably, sodium vanadate is able to induce PE differentiation in inner cells of ES cell aggregates which occurs only in the outer layer in the absence of sodium vanadate[51]. In addition, sodium vanadate alters mRNA expression in downstream Nanog targets, where PE marker Gata-6 is increased and pluripotency

gene Rex1 is downregulated, and these changes in gene expression can be prevented by *Nanog* overexpression[51]. In contrast to wild-type ES cells, *Grb2* null ES cells treated with sodium vanadate do not downregulate *Nanog* or differentiate to PE[51]. Similarly, Mek inhibition with PD98059 and sodium vanadate treatment prevents PE differentiation while PI3K or Jnk inhibitors do not[51]. Also, constitutive activation of Mek induced differentiation to PE and repressed *Nanog* transcription, while a kinase dead Mek 1 mutant was insufficient to mediate these changes[51]. These data establish a clear role for the Mek/Erk pathway in repression of *Nanog* and differentiation to the PE lineage.

Nanog Transcriptional Regulation

Currently, two major *cis*-regulatory regions have been implicated in the control of *Nanog* gene expression: the proximal promoter region and the distal enhancer region (Figure 1-2). Oct4 and Sox2 proteins or Oct4 and Sox binding protein (SBP) bind to each other and to the *Nanog* promoter less than 200 bp upstream of the transcription start site, and are necessary and sufficient for transcription[46, 47]. FoxD3 is thought to act as a positive activator of *Nanog* to oppose the repressive effects of high levels of Oct4[52]. Recently, Zfp143 has been shown to regulate *Nanog* levels by altering Oct4 binding to the promoter[53]. The distal region is additionally bound by positive regulators which enhance *Nanog* expression. These include STAT3 and T[54], Klfs[55], and Nanog/Sall4[56].In addition, a small number of negative regulators of *Nanog* expression have been identified which bind outside of these two regulatory regions.

These negative regulators include p53, GCNF, and Tcf3. Tcf3, one of the DNA-binding transcriptional regulators of the Wnt pathway, is the most highly expressed Tcf proteins in undifferentiated ES cells, and null ES cells displayed delayed differentiation and elevated *Nanog* mRNA and protein expression[57]. Tcf3 was shown to bind to the

Nanog promoter and reduce *Nanog* expression levels, which the authors hypothesize helps maintains ES cell self renewal by moderating autoregulation of Nanog, Oct4, and Sox2[57]. GCNF has been shown to repress pluripotency genes including *Nanog* and Oct4 during retinoic acid induced differentiation[58].Finally, p53 activation following DNA damage has been shown to suppress *Nanog* expression through recruitment of the co-repressor mSin3a to the *Nanog* promoter[59].

Nanog expression is not homogeneous in mouse ES cell culture. Indeed, ES cells can be divided into two populations: Nanog-high cells and Nanog-low cells[60]. Interestingly, Nanog-low cells express the PE marker Gata6, a pattern which is seen in ICM mass cells of the early blastocyst stage embryo[60]. This indicates that ES cells serve as a good model system for understanding early embryonic development. In addition, Nanog controls Gata6 expression by binding to the Gata6 promoter region where it acts to prevent Gata6 expression[60]. Interestingly, overexpression of Nanog is able to reduce heterogeneity during ES cell maintenance[60].

Significance

ES cells serve as a model system for preimplantation development and their properties of self-renewal and pluripotency allow scientists to study molecular mechanisms involved in both maintaining pluripotency and inducing differentiation. Though scientists have come a long way in their understanding of extrinsic and intrinsic factors that balance self-renewal and differentiation, it is currently unclear how expression of core transcriptional factors including Oct4, Sox2, and Nanog are controlled. Though *in vivo* and *in vitro* work has demonstrated the importance of FGF/FGFR interaction and activation of the downstream MAPK signaling pathway through Mek/Erk is vital for PE differentiation, it is currently unclear how this signaling

ultimately represses *Nanog*. The overall goal of this study is to determine the mechanism of FGFR-mediated *Nanog* repression. This will increase our understanding of the transcriptional regulatory networks in ES cells which control pluripotency and differentiation, which will have important implications in cell fate specification in the early embryo.

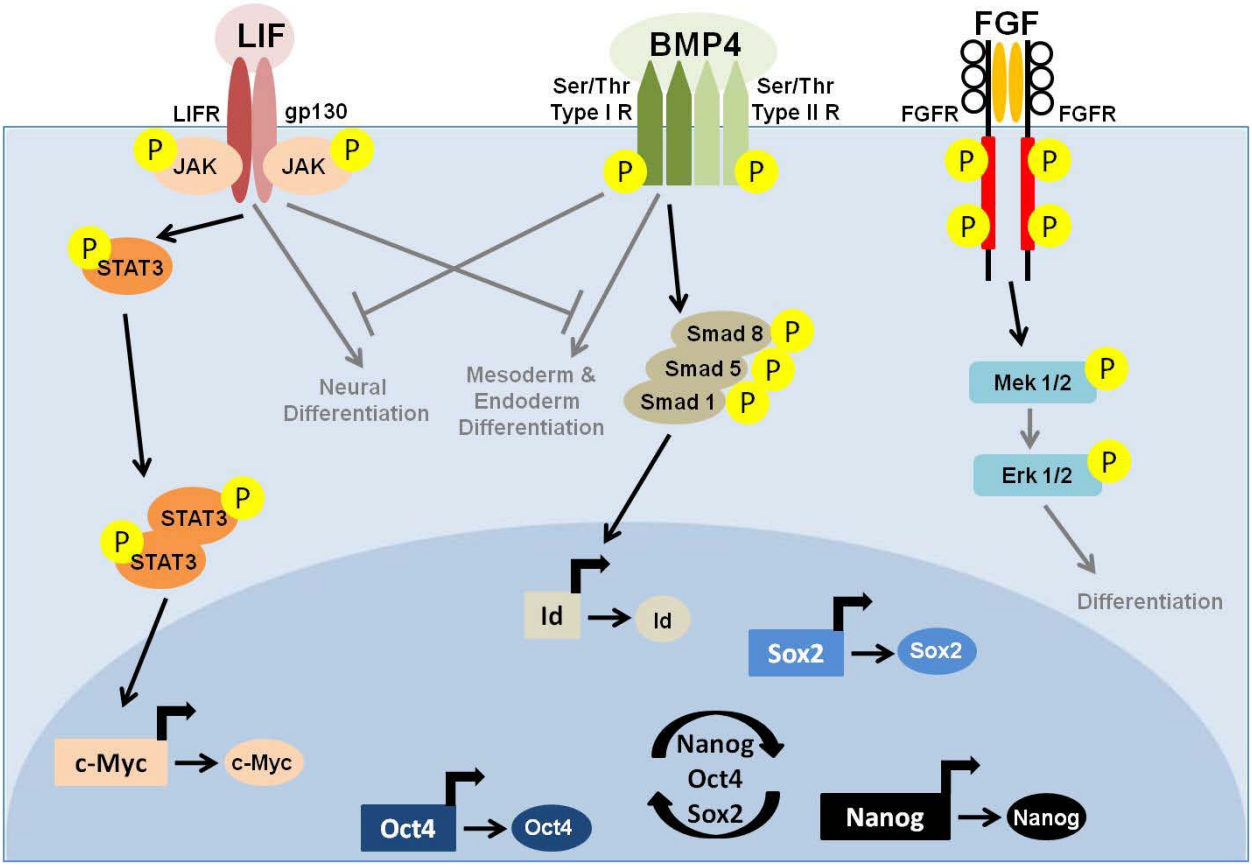

Figure 1-1. Signaling pathways involved in maintaining mouse ES cell pluripotency and promoting differentiation. LIF mediates its pro-pluripotency effects by activation of JAK/STAT, and STAT phosphorylation induces dimerization and translocation to the nucleus to act on genes including c-Myc, and prevent mesoderm and endoderm differentiation. BMP4 acts through Smads1,5, and 8, which translocate to the nucleus upon phosphorylation, and act on genes including Id genes to prevent neural differentiation. Oct4, Sox2, and Nanog form a feed forward loop to maintain ES cells in an undifferentiated state. In contrast, FGF/FGFR activation results in Mek/Erk phosphorylation which leads to differentiation.

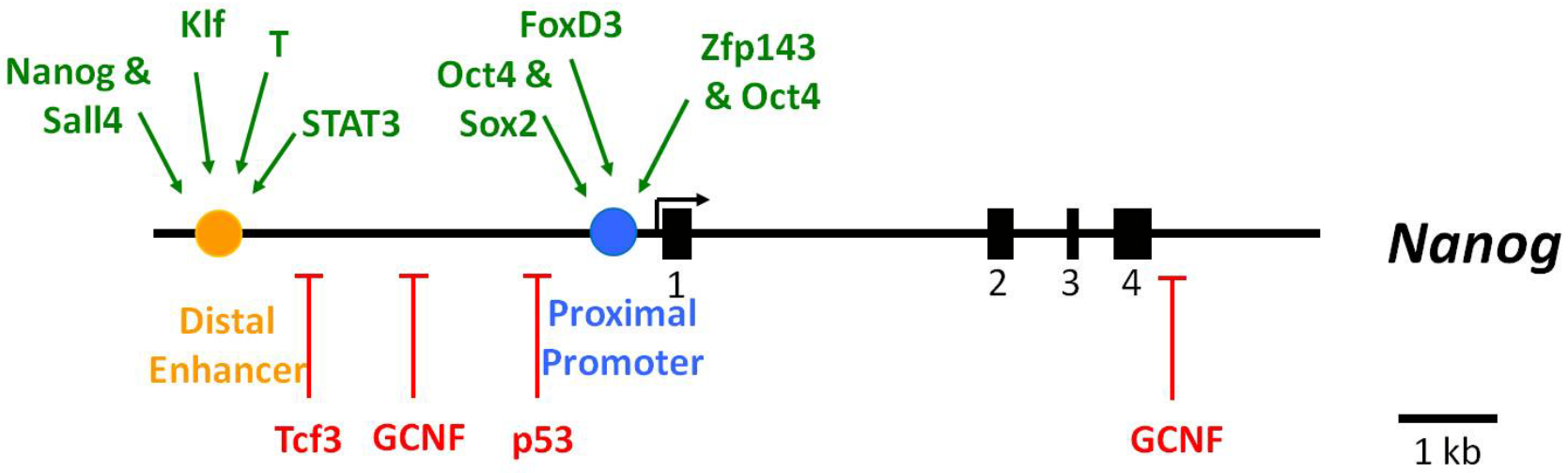

Figure 1-2. *Nanog* transcription in regulated by a multitude of factors. The *Nanog* gene locus encodes 4 exons and its expression is positively controlled primarily by two *cis*-regulatory regions: the distal enhancer approximately 5 kb upstream and the proximal promoter region located near the transcription start site. Oct4 and Sox2 transcription factors are required and sufficient for *Nanog* transcriptional activation. FoxD3, Zfp143, Nanog, Sall4, Klf, T, and STAT3 have been demonstrated to positively influence *Nanog* transcription. In contrast, Tcf3, GCNF, and p53 have been shown to limit *Nanog* transcription

CHAPTER 2
MATERIALS AND METHODS

Murine Embryonic Stem Cell Culture

Murine ES cells were maintained in an undifferentiated state on gelatin-coated cell culture dishes in Knockout Dulbecco's Modified Eagle Medium (KO DMEM; Gibco, Grand Island, NY) supplemented with 10% Knockout Serum Replacement (KSR; Gibco), 1% fetal bovine serum (FBS; Atlanta Biologicals, Norcross, GA), 2 mM L-glutamine, 100 units/ml penicillin, 100 μg/ml streptomycin, 25 mM HEPES (Mediatech, Manassas, VA), 300 μM monothioglycerol (MTG; Sigma, St. Louis, MO), and 1000 units/ml recombinant mouse Leukemia Inhibitory Factor (LIF) (ESGRO; Chemicon, Temecula, CA). ES cells were maintained at 37°C in 5% CO_2.

Fibroblast Growth Factor Receptor 2 Plasmid Construction and Stable Cell Line Creation

We generated transgenic ES cells with inducible FGFR2 activation system using the Argent Regulated Homodimerization Kit (Ariad Pharmaceuticals Inc., Cambridge, MA). The portion of the $pC_4M\text{-}F_v2E$ plasmid containing a myrisotoylation signal, two tandem FK506 binding domains (FKBP36V), and a c-terminal hemagglutinin (HA) tag was digested using EcoRI and BamHI restriction enzymes. The digested region was then ligated into the pCAG-IRES-Hyg plasmid using EcoRI and BamHI restriction sites. This modified plasmid allows for constitutive expression in ES cells driven by the chicken β-actin promoter and provides a hygromycin-resistance gene for clonal selection. The cytoplasmic domains of FGFR2 were PCR amplified using the forward primer 5'-GACTAGTATGAAGACCACGACCAAGAAGC- 3' and the reverse primer 5'-GCTCTAGATGTTTTAACACTGCCGTTTATGT-3'. Following amplification, the PCR

fragment was digested with SpeI and ligated in-frame into the SpeI site of the pCAG-F36V-IRES-Hyg vector at the C-terminal end of the F36V domain. R1 ES cells were transfected with the pCAG-F36V-IRES-Hyg, and were selected with hygromycin (200 μg/ml) for two weeks and individual clones were isolated and expanded.

Plasmid Construction

Luciferase reporter plasmids were constructed following Kuroda et al (2005)[47] with minor modifications. Fragments from the mouse *Nanog* gene promoter were amplified from the mouse genome using a common reverse primer containing an SpeI restriction site (+50 bp from the transcription start site, 5'-GGACTAGTCGCAGCCTTCCCACAGAAA-3') and one of three forward primers to create 2,342 bp, 332 bp, and 153 bp reporters (-2,342 bp: 5'-ATTTGCGGCCGCTGGTGTAAACAGTG-3'; -332 bp: 5'-ATTTGCGGCCGCATCGCCAGGGTCTGGA-3'; -153 bp: 5'-ATTTGCGGCCGCCCTGCAGGTGGGATTAACT-3'). The PCR amplified products were digested using NotI and SpeI restriction enzymes and ligated into the NotI and SpeI sites of pGL2-Basic (Promega Corporation, Madison, WI).

Luciferase reporter plasmids containing insulator elements were constructed using two copies of the 1.2 kb chicken β-globin core HS4 insulator taken from the pJC13-1 plasmid. First, pJC13-1 was cut with the SalI restriction enzyme. Next, to make a blunt end, 1 μl of dNTP mix (10 mM each) and 2 μl T4 DNA polymerase (New England Biolabs) was added to the SalI digestion reaction, and incubated for 20 minutes at 12°C. The reaction was heat inactivated for 10 minutes at 75°C, and the plasmid was purified using QIAquick PCR Purification Kit (QIAGEN). The SalI/blunt ended pJC13-1 plasmid

was next digested with the BamHI restriction enzyme to free the 2.4 kb HS4 insulator. The pENTR/H1/TO plasmid (Invitrogen) containing zeocin and kanamycin resistance genes was digested with BglII and EcoRV to prepare for ligation of the HS4 insulator. Next, the BamHI digested end was ligated to the cohesive compatible end BglII, while the SalI-digested blunted end was ligated to the blunt end provided by EcoRV digestion to create the plasmid pHS4-Zeo. To insert a luciferase reporter driven by *Nanog* promoter activity, the previously constructed *Nanog* -332 bp pGL2-Basic reporter was first digested with the KpnI restriction enzyme. After purification using the QIAquick PCR Purification Kit (QIAGEN), the plasmid was digested with BamHI and PvuI. The 3.1 kb fragment containing the *Nanog* promoter and luciferase reporter was gel purified using the QIAquick Gel Extraction Kit (Qiagen), while the 1 kb and 1.5 kb bands were discarded. The plasmid pHS4-Zeo was digested with KpnI and BamHI, and the 3.1 kb insert was ligated to generate p5'HS4-330Luc-Zeo. Subsequent reporters with varying promoters were easily constructed by digesting p5'HS4-330Luc-Zeo with SpeI NotI and PCR amplifying promoter inserts with an SpeI restriction site in the forward primer and a Not1 restriction site in the reverse primer.

Plasmids were constructed according to the following procedures. First, inserts were generated by polymerase chain reaction (PCR) using LA-*Taq* polymerase (Takara Mirus Bio, Madison, WI). Each PCR reaction contained the following components: 10 ng DNA template, 1.5 μl forward primer (100 μM stock), 1.5 μl reverse primer (100 μM stock), 10 μl LA PCR buffer II (10x), 2 μl dNTP mix (2.5 mM each), 0.5 μl LA Taq (5 U/μl), and autoclaved dH_2O in a final reaction volume of 100 μl. PCR conditions

were as follows: 95°C 1 minute, 20 cycles of 98°C 5 seconds and 68°C 5 minutes, followed by 72°C for 10 minutes.

PCR reactions were purified using the QIAquick PCR Purification Kit (Qiagen Sciences, Germantown, MD). Briefly, 500 μl Buffer PB was added to each PCR reaction and mixed. DNA was bound to the spin column by centrifugation for 30 seconds at 13,000 rpm at room temperature. DNA was washed with 750 μl Buffer PE by centrifugation for 30 seconds at 13,000 rpm at room temperature, and was eluted with 50 μl Buffer EB by centrifugation for 1 minute at 13,000 rpm at room temperature.

For cloning, purified PCR products and plasmids were digested using appropriate restriction enzymes to create compatible ends. Digestion reactions included 42.5 μl purified PCR product, 5 μl appropriate NEBuffer (New England Biolabs Inc, Beverly, MA), 0.5 μl bovine serum albumin (BSA) if required, 1 μl restriction enzyme #1, 1 μl restriction enzyme #2 (New England Biolabs) in a total volume of 50 μl. For plasmid digestion, 10-15 μg was digested following the above reaction setup, and an appropriate volume of autoclaved dH_2O was added for a final reaction volume of 50 μl. Digestion reactions were incubated overnight at 37°C. The next morning, digestion enzymes were heat inactivated by incubation for 20 minutes at 65°C.

Digested DNA was gel purified using 1-2% agarose/TBE (0.5x) ethidium bromide stained gels. DNA bands were cut using a clean scalpel blade, and DNA was purified using QIAquick Gel Extraction Kit (Qiagen). Briefly, gel slices were dissolved in 3 volumes Buffer QG to 1 volume (by weight) of gel by incubation for 10 minutes at 50°C. DNA was bound to spin column by centrifugation for 1 minute at 13,000 rpm at room temperature. To wash DNA, 750 μl Buffer PE was added and centrifuged for 1

minute at 13,000 rpm at room temperature. DNA was eluted in 50 μl Buffer EB by centrifugation for 1 minute at 13,000 rpm at room temperature.

Insert and plasmid DNA concentrations were measured by spectrophotometry at an absorbance of 260 nm, where an A260 reading of 1 equals a DNA concentration of 50 μg/ml. DNA with an A260/280 ratio between 1.8 and 2.0 was considered to be of high purity. For ligations, a 3 to 1 insert to vector molar ratio was calculated for a total ligation reaction volume of 5.5 μl. Reaction components were prepared as follows: 4 μl DNA (vector plus insert), 1 μl 5x T4 DNA Ligase Buffer (Invitrogen), and 0.5 μl T4 DNA Ligase (Invitrogen). Components were mixed and incubated overnight at 16°C.

Transformations were performed using Max Efficiency DH5a *E. coli* chemical competent cells (Invitrogen). To begin, a 40 μl aliquot of *E.coli* was thawed on ice. Next, 2 μl of the ligation reaction was added to cells, mixed by gentle tapping, and placed on ice for 30 minutes. Next, cells were heat-shocked for 45 seconds at 42°C, placed on ice for 2 minutes, and after removing cells from ice, 950 μl of Super Optimal broth with Catabolite repression (SOC) medium was added to each transformation reaction. Cells were incubated for 1 hour in a shaking incubator at 200 rpm at 37°C. Next, 100 μl of the transformation reaction was spread onto pre-warmed Luria-Bertani (LB) agar plates containing either ampicillin or kanamycin antibiotics (50 μg/ml), and bacterial plates were incubated overnight upside-down at 37°C. The next day, colonies were picked up and grown in 2 ml of LB medium containing appropriate antibiotic (50 μg/ml) overnight in a shaking incubator at 200 rpm at 37°C.

Transformed plasmids were isolated from bacteria using QIAprep Spin Miniprep Kit (Qiagen). Briefly, bacterial cells were centrifugation for 1 minute at 13,000 rpm at

room temperature. Bacteria pellet was resuspended in 250 μl Buffer P1, 250 μl Buffer P2 was added for cell lysis, and sample was mixed by inverting the tube 4-6 times. Neutralization was accomplished by addition of 350 μl Buffer N3 followed by inverting tube another 4-6 times. Centrifugation for 10 minutes at 13,000 rpm at room temperature pellets bacterial cell components, at supernatant was added to a spin column to bind DNA. DNA was washed with 750 μl Puffer PE by centrifugation for 1 minute at 13,000 rpm, and purified DNA was eluted with 50 μl Buffer EB by centrifugation for 1 minute at 13,000 rpm at room temperature.

To confirm successful ligation, purified plasmid DNA was digested for 1 hour with a slight modification of the digestion reaction volume and conditions previously described above. Digestion reactions were prepared as follows: 10 μl purified plasmid DNA, 6.8 μl autoclaved dH_2O, 0.5 μl restriction enzyme #1, 0.5 μl restriction enzyme #2, 2 μl appropriate NEBuffer, and 0.2 μl BSA. Reactions were incubated for 2 hours at 37°C, and subsequently analyzed by agarose gel electrophoresis as described above. DNA sequencing was performed to confirm that no DNA mutations occurred during PCR synthesis. Sequencing reaction was performed using BigDye Terminator v3.1 Cycle Sequencing Kit (Applied Biosystems Inc., Foster City, CA). Briefly, 4 μl Big Dye Terminator 3, 2 μl 5x sequencing buffer, 3.2 pmoles sequencing primer, and 200-500 ng plasmid DNA were mixed. PCR sequencing reaction contained the following steps: 25 cycles of 96°C for 30 seconds, 50°C for 15 seconds, 60°C for 4 minutes.

DNA was purified by isopropanol precipitation. Briefly, 20 ml of autoclaved dH_2O and 60 ml 100% isopropanol were added to the sequencing reaction, and the sample was mixed briefly by vortex. Following incubation for 20 minutes at room temperature,

samples were centrifuged for 20 minutes at 13,000 rpm at 4°C. Supernatant was aspirated immediately and 250 μl 75% isopropanol was added. Sample was mixed briefly by vortex and centrifuged for 5 minutes at 13,000 rpm at 4°C. Supernatant was aspirated and remaining isopropanol was removed from sample by incubation for 1 minute in a 90°C heating block.

Plasmids without mutations were expanded by transformation as described above and colonies were picked up and grown in 50 ml LB medium containing appropriate antibiotics (50 μg/ml) overnight in a 37°C incubator shaking at 200 rpm. The next morning, plasmid DNA was purified using NucleoBond Xtra Midi Kit (Macherey-Nagel, Düren, Germany). Briefly, bacterial cells were centrifuged for 15 minutes at 4,100 rpm. The cell pellet was resuspended in 8 ml of Buffer RES, and cells were lysed by incubation of 8 ml Buffer LYS for 5 minutes at room temperature. Lysis was neutralized by addition of 8 ml of Buffer NEU, and lysate was added to the column filter. Next, the filter was washed with 8 ml Buffer EQU, and the filter was removed from the column and discarded. A second wash step was accomplished with 8 ml of Buffer WASH, and purified DNA was eluted from the column with 5 ml of Buffer ELU. DNA was purified by DNA purification as follows: 3.5 ml 100% isopropanol was added to the eluate and sample was centrifuged for 30 minutes at 12,700 rpm at 4°C. The supernatant was discarded, and the DNA pellet was washed in 2 ml 70% ethanol, followed by centrifugation for 5 minutes at 12,700 rpm at 4°C. After aspirating the supernatant, the DNA pellet was dried at room temperature for 5-10 minutes. DNA was reconstituted in autoclaved dH_2O by incubation on a rocking platform overnight at 4°C.

RNA Isolation and cDNA Synthesis

For reverse-transcription polymerase chain reaction (RT-PCR), total RNA was extracted using the RNAqueous kit (Ambion, Austin, TX). Briefly, growth media was removed from cell culture dishes by aspiration and cells were washed with calcium and magnesium-free sterile Dulbecco's Phosphate Buffered Saline (DPBS; Mediatech). Lysis/Binding solution and an equal volume of 64% ethanol was added to the washed cells. The cell lysate was gently mixed with a pipette, added to the filter cartridge, and centrifuged for 30 seconds at 12,000 rpm at 4°C. The filter was washed three times, first with 700 μl Wash Solution 1, then two times with 500 μl Wash Solution 2, with centrifugation in between washes. To elute RNA, 35 μl Elution solution was incubated with the filter for 2 minutes, and cartridges were spun for 1 minute at 12,000 rpm at room temperature.

To remove contaminating DNA from the RNA preparation, we used the TURBO DNA-free Kit (Ambion). Briefly, 30 μl of RNA was incubated with 0.5 μl DNase (2 Units) and 3 μl 10x DNase buffer at 37°C for 20 minutes. Next, 3 μl of inactivation reagent was added, and sample was incubated at room temperature for 2 minutes with occasional tapping. Finally, the sample was centrifuged for 2 minutes at 13,000 rpm and 20 μl of the supernatant containing RNA was transferred to a clean tube.

First-strand cDNA synthesis was carried out using the High Capacity cDNA Reverse Transcription Kit using random primers (Applied Biosystems, Foster City, CA). Briefly, we prepared a 20 ml reaction volume to convert up to 2 μg of RNA as follows: 2 μl 10x RT buffer, 1 μl dNTPs (100 mM each), 2 μl random primers, 1 μl MultiScribe RTase, 10 μl DEPC- dH_2O, and up to 4 μl RNA (up to 2 μg). The PCR reaction

consisted of the following incubation steps: 25°C for 10 minutes, 37°C for 120 minutes, and 85°C for 5 seconds. Next, using dH_2O, cDNA was diluted to 5 ng/μl based on starting RNA concentration, and samples were stored at -20°C.

Real-Time Quantitative Polymerase Chain Reaction

Real-Time quantitative polymerase chain reaction (qPCR) was performed using Power SYBR Green dye (Applied Biosystems). To prepare samples, cDNA was diluted from 5 ng/μl to 0.5 ng/μl in autoclaved dH_2O. Primers were designed using Primer3 software [61] to conform to general guidelines suggested in the SYBR Green PCR Master Mix Protocol (Applied Biosystems): primer length of 20bp, GC content between 30 and 60%, T_m between 58 and 60°C, with a 125-150 bp amplicon size. Primer mixes were prepared to a final concentration of 2 mM (each primer) by diluting 50 μM forward primer stock with 50 μM reverse primer in dH_2O. Each 20 μl PCR reaction consisted of 10 μl Power SYBR green PCR master mix (Applied Biosystems), 5 μl of primer mix (2 uM each primer), and 5 μl 0.5 ng/ul cDNA . Samples were run in duplicate or triplicate and standard curves were generated for each primer set on each PCR run. To prepare standard curves, 5 ng/ul cDNA was serially diluted to 1:2, 1:4, 1:8, 1:16, 1:32, and 1:64 in autoclaved dH_2O. Reactions were performed on the MJ Research DNA Engine Opticon 2 real-time PCR instrument using Opticon Monitor 3.1.32 software (Bio-Rad Laboratories, Hercules, CA). Gene expression analysis was performed using the comparative CT method using β-actin for normalization. Primer sequences are listed in Table 2-1.

Immunoblotting

ES cells were grown in 6-well cell culture dishes for 4 days prior to harvesting. Cells were lysed in 100 μl radioimmunoprecipitation assay (RIPA) buffer (50 mM Tris-Cl pH 7.4, 150 nM NaCl, 1% NP-40, 0.25% Na-deoxycholate, and protease inhibitors) on ice for 10 minutes. The cells were then removed from the plate using a cell scraper, and the cell lysate was incubated on ice for 30 minutes. Cell lysate protein concentrations were determined by D_C Protein Assay (Bio-Rad), and 10 μl of lysate per lane was separated through 12% polyacrylamide by sodium dodecyl sulfate (SDS)-polyacrylamide gel electrophoresis using mini-PROTEAN TGX precast gels (Bio-Rad). Proteins were transferred to a 0.2 mm nitrocellulose Ready Gel Blotting Sandwich membrane (Bio-Rad). Blocking was performed with 4% BSA in Tris-Buffered Saline Tween-20 (TBST; 100 mM NaCl, 50 mM Tris, 0.05% Tween-20 pH 7.5) on a shaking platform for 1 hour at room temperature. Membranes were incubated with anti-Nanog (1:1,000 dilution; AB5731; Chemicon), Oct4 (1:1,000 dilution; C-10; Santa Cruz), Sox2 (1:1,000 dilution; H-65; Santa Cruz), phospho-Erk1/2 (1:1,000 dilution; E10; Cell Signaling), or β-Actin (1:1,000 dilution; 13E5; Cell Signaling) overnight at 4°C. Washing was performed withTBST and membranes were incubated with horseradish peroxidase-conjugated immunoglobulin G (1:5,000 dilution; Santa Cruz) for secondary antibody. Proteins were visualized using enhanced chemiluminescence (ECL) detection (Pierce, Thermo Scientific).

Anti-phosphotyrosine (9411; Cell Signaling) and β-actin (4967; Cell Signaling) blot and multiplex blot using anti-phospho-90RSK, phosphor-Akt, phosphor-Erk1/2, phosphor-S6, and eIF4E immunoblots (5301; Cell Signaling) were performed by Cell

Signaling Technology using 30 ug/lane of protein on a 4-20% gradient gel. Blots were developed using LI-COR Odyssey near infrared imaging system.

Chromatin Immunoprecipitation

R1 ES cells were plated on 10 cm cell culture dishes at an appropriate density to yield 5 x 10^6 cells per dish on day four. One day prior to harvesting cells, we prepared blocked recombinant Protein G-Sepharose 4B Conjugate beads (Invitrogen, Grand Island, NY). Blocking buffer was freshly prepared by combining 3 ml ChIP dilution buffer (0.01% SDS, 1.1% Triton X-100, 1.2 mM ethylenediaminetetraacetic acid (EDTA), 16.7 mM Tris-Cl pH 8.0, and 167 mM NaCl), 150 μl of 20 mg/ml bovine serum albumin (BSA) fraction V (Fisher Scientific, Pittsburgh, PA), and 30 μl of 10 mg/ml sonicated salmon sperm DNA (Stratagene, Cedar Creek, TX). To remove protein G-sepharose storage buffer, a 1 ml slurry of Protein G-sepharose was mixed with 5 ml of ChIP dilution buffer, centrifuged for 2 minutes at 1,000 rpm at 4°C, and supernatant was discarded. Next, 2.5 ml of blocking buffer was added, and Protein G-sepharose was incubated overnight at 4°C on a rocking platform. The next day, the protein G-sepharose in blocking buffer was centrifuged for 2 minutes at 1,000 rpm at 4°C, supernatant was discarded, and 500 ml of blocking buffer was added. Blocked protein G-sepharose was stored at 4°C until use.

To begin ChIP, formaldehyde was added to cell culture media to a final concentration of 1% and incubated at room temperature for 10 minutes on a rotating platform. Next, crosslinking was stopped by addition of 125 mM glycine to the culture dishes for 5 minutes on a rocking platform at room temperature. Next, media was removed and dishes were washed twice with ice-cold PBS supplemented with EDTA-

free SIGMAFAST Protease Inhibitor (PI) Cocktail (Sigma). Cells were then removed from the dish by scraping in PBS containing PIs on ice, and collected by centrifugation for 5 minutes at 1200 rpm at 4°C. Supernatant was discarded, and cell pellets from 4 cell culture dishes (at approximately 5 million cells each) were combined for a total of approximately 2 x 10^7 million cells in 1 ml ChIP cell lysis buffer (5 mM PIPES pH 8.0, 85 mM KCl, 0.5% NP-40, and PIs). Cells were gently mixed by pipette to remove clumps, and were allowed to lyse for 10 minutes on ice. Nuclei were pelleted by centrifugation for 5 minutes at 5,000 rpm at 4°C, and the supernatant was discarded. Next, nuclei were lysed in 800 μl ChIP nuclei lysis buffer (50 mM Tris-Cl pH 8.1, 10 mM EDTA, 1% SDS, and PIs) for 10 minutes on ice. Next, chromatin was sheared to a size of 200-1000 bp, with an average of 500 bp on ice using a Fisher Scientific Sonic Dismembrator Model 100 (Fisher Scientific). In general, 10 pulses of 10 seconds of sonication at a power setting of "4" with a 1 minute rest between pulses was sufficient to shear chromatin to the desired size. Next, sonicated samples were centrifuged for 10 minutes at 13,000 rpm at 4°C to pellet debris. Supernatant was transferred to a clean tube and diluted (1:10) up to 8 ml total volume in ChIP dilution buffer. Chromatin was precleared by addition of 60 ml blocked protein G (per 8 ml sample of diluted chromatin) for 20 minutes on a rocking platform at 4°C. Chromatin was centrifuged for 3 minutes at 1,000 rpm at 4°C to pellet protein G-sepharose. Supernatant was transferred to a clean tube, and 100 ul was set aside at 4°C to serve as an input control. Next, 2 ml of chromatin was divided for each immunoprecipitation, 2-4 μg of antibody was added, and samples were incubated overnight on a rocking platform at 4°C. Antibodies used for ChIP can be found in Table 2-2.

The next day, 60 ml of blocked protein G-sepharose was added to each sample, and incubated for 1 hour at 4°C. Samples were centrifuged for 2 minutes at 1,000 rpm at 4°C, and supernatant was carefully discarded. Pelleted beads were washed seven times with 1 ml ChIP LiCl wash buffer (0.25 M LiCl, 0.5% NP-40, 0.5% deoxycholic acid sodium salt (DOC), 1 mM EDTA, and 10 mM Tris-Cl pH 8.0) followed by centrifugation for 1 minute at 2,500 rpm at 4°C between washes. After the fifth wash, protein G-sepharose beads were incubated with 1 ml wash buffer for 10 minutes on a rocking platform at 4°C to reduce background. After the final wash, the last traces of buffer were removed using a clean 1 ml syringe with 27G needle. To elute DNA: protein complexes from the protein G-sepharose, 100 μl of ChIP elution buffer (50 mM Tris-Cl pH 8.0, 1% SDS, and 10 mM EDTA) was added to the samples, and they were taped on a Vortex Genie 2 (Fisher Scientific) to shake on level 3 for 15 minutes at room temperature. After vortexing, samples were centrifuged for 1 minute at 3,000 rpm at room temperature, and the supernatant was transferred to a clean tube. A second elution step was carried out by addition of 150 μl ChIP elution buffer, 15 minutes shaking on the vortex, centrifugation, and the supernatant was added to the tube containing the first eluate. To reverse crosslinking, 10 ul of 5 M NaCl was added to the eluate, and incubated overnight at 65°C. To prepare the input sample, 20 μl of chromatin previously stored at 4°C was diluted with 250 μl elution buffer, 10 μl of 5M NaCl was added, and samples were incubated overnight at 65°C.

The next morning, proteins were degraded with 1 μl proteinase K (20 mg/ml) and samples were incubated for 2 hours at 55°C. To extract DNA, an equal volume (250 ml) of phenol:chloroform was added, and the samples were mixed by vortex for 20 seconds

followed by a second vortex of 20 seconds. Samples were centrifuged for 5 minutes at 13,000 rpm at room temperature, and the top layer was transferred to a clean tube. DNA was purified using the QIAquick PCR Purification Kit (QIAGEN Sciences, Germantown, MD). Briefly, 1000 μl Buffer PB was added to each sample, and sample was added to spin column. DNA was bound to column by centrifugation for 30 seconds at 13,000 rpm at room temperature. DNA was washed with 750 μl Buffer PE by centrifugation for 30 seconds at 13,000 rpm at room temperature, and was eluted with 50 ml Buffer EB by centrifugation for 1 minute at 13,000 rpm at room temperature.

PCR was performed using quantitative real-time PCR as described above with slight modifications to DNA samples. Each IP sample was diluted 1:5 in autoclaved dH_2O , while Input samples were diluted 1:50 in autoclaved dH_2O. Standard curves for each primer set were prepared by generating serial dilutions of Input DNA (1:10, 1:100, 1:1,000, and 1:10,000). Primer sequences used for real-time PCR analysis for ChIP can be found in Table 2-3. Each sample (IP and Input) was run in triplicate for each primer set. Protein binding enrichment was analyzed by calculating % input.

Reporter Assays

FGFR2 R1 ES cells were plated at a density of 6×10^4 cells per well in a 6-well plate (9.5 cm^2 growth area). After 24 hours, cells were transfected using FuGENE 6 Transfection Reagent (Roche Diagnostics, Indianapolis, IN). All steps were carried out in a sterile cell culture hood. Briefly, 100 μl OPTI-MEM 1 reduced serum medium (Invitrogen) and 6 μl FuGENE 6 were combined, gently mixed by taping, and incubated for 10 minutes at room temperature. Next, 2 μg total DNA was added, and samples were incubated for 20 minutes at room temperature. Following incubations, transfection

reaction was added dropwise to the cells in the designated well of a 6-well plate. Medium was changed 24 hours post transfection.

Transient Transfection Reporter Assays

Luciferase reporter constructs were transfected as described above using 2.0 μg DNA luciferase reporter vector co-transfected with 0.2 μg pRL-TK-*Renilla* internal control vector (Promega Corporation, Madison, WI). Forty-eight hours post transfection, cells were harvested with the Dual- Luciferase reporter assay system (Promega) using 100 μl Passive Lysis Buffer (1x) and a cell scraper. Cell lysates were subjected to two freeze-thaw cycles at -80°C. Luciferase activities were measured using a Moonlight 2010 luminometer (Analytical Luminescence Laboratory, San Diego, CA). Briefly, 100 μl Luciferase Assay Reagent II was combined with 20 μl cell lysate in a 12 x 75 mm borosilicate glass Disposable Culture Tube (Fisher Scientific), and mixed by gently tapping. Firefly luciferase activity was measured, the signal was quenched and *Renilla* luciferase activity was activated by addition of 100 μl Stop and Glo Reagent. Luciferase activity was calculated in relative luciferase units (RLU) determined by the ratio of firefly luciferase to *Renilla* luciferase times 1,000, which allows for normalization based of transfection efficiency measured by *Renilla* luciferase activity. Promoter activity is reported as mean ± standard error.

Stable Transfection Reporter Assays

Insulated luciferase reporter constructs were digested with NheI, and transfections were carried out as described above using 2 μg DNA luciferase reporter vector co-transfected with the puromycin resistant selectable vector pCAG ER Puro. ES cells were selected with 1.25 μg/ml of puromycin for 14 days and individual colonies were

manually picked up and transferred to a 24-well plate. After expansion of individual clones, cells were plated at 6 x 10^4 cells per well in a 6-well cell culture dish, and treated with AP0127 for 0,6,or 24 hours. Total RNA was extracted from cells and cDNA was synthesized as described above. Real-time PCR was carried out as described using primers specific for endogenous Nanog, luciferase, or β-actin gene expression.

Table 2-1. Forward and reverse primers used for real-time PCR

Primer Name	Sequence (5' to 3')	Amplicon size (bp)
β-actin Forward	TGACAGGATGCAGAAGGAGA	99 bp
β-actin Reverse	CCACCGATCCACACAGAGTA	
Nanog Forward	CTGCTCCGCTCCATAACTTC	97 bp
Nanog Reverse	GCTTCCAAATTCACCTCCAA	
Luciferase Forward	TGGGTTACCTAAGGGTGTGG	103 bp
Luciferase Reverse	CGCAGTATCCGGAATCATTT	
Oct4 Forward	AGAACCGTGTGAGGTGGAGT	85 bp
Oct4 Reverse	TGATTGGCGATGTGAGTGAT	
Sox2 Forward	CTCTGCACATGAAGGAGCAC	91 bp
Sox2 Reverse	CCGGGAAGCGTGTACTTATC	
Gata6 Forward	ATCACCATCACCCGACCTAC	100 bp
Gata6 Reverse	CCCTGTAAGCTGTGGAGCAC	
β-geo Forward	CTCGACGTTGTCACTGAAGC	100 bp
β-geo Reverse	ATACTTTCTCGGCAGGAGCA	
Nanog Pre-mRNA Forward	CATGTTTAAGGTCGGGCTGT	116 bp
Nanog Pre-mRNA Reverse	GCTTGCACTTCATCCTTTGG	
Oct4 Pre-mRNA Forward	GTCCCAGCTGGTGTGACTCT	109 bp
Oct4 Pre-mRNA Reverse	TCTTCTGCTTCAGCAGCTTG	

Table 2-2. Antibodies used in chromatin immunoprecipitation

Antibody	Company	Amount used per IP
H3K4me3	Millipore (07-473)	2 μg
H3K9me3	Abcam (ab8898)	2 μg
H3K27me3	Millipore (17-622)	2 μg
H3K36me3	Abcam (ab9050)	2 μg
RNA Polymerase II (phospho S5)	Abcam (ab5131)	2 μg
p300 (N-15)	Santa Cruz (sc-584)	2 μg
GKlf (Klf4) (T-16)	Santa Cruz (sc-12538)	2 μg
Sox-15 (T-20)	Santa Cruz (sc-17354)	2 μg
Sox-2 (Y-17)	Santa Cruz (sc-17320X)	2 μg
Oct-3/4 (N-19)	Santa Cruz (sc-8628X)	2 μg

Table 2-3. Chromatin immunoprecipitation real-time PCR primers

Primer Region	Sequence (5' to 3')	Amplicon size (bp)
Nanog -1589 Forward	CAGTGGAAGAAGGGAAGTGG	142 bp
Nanog -1447 Reverse	ACTGCACCACACCATCATTG	
Nanog -221 Forward	CTTTCCCTCCCTCCCAGTCT	164 bp
Nanog -57 Reverse	TCAAGCCTCCTACCCTACCC	
Nanog -87Forward	GAGAATAGGGGGTGGGTAGG	160 bp
Nanog +76 Reverse	CAAGAAGTCAGAAGGAAGTGAGC	
Nanog +932 Forward	CTCTGTGTAGCCCTGGCTGT	150 bp
Nanog +1082 Reverse	CTATCCCCACCCGTTCATTC	
Nanog +2006 Forward	TGAAAGGTCCCAACAGGATT	155 bp
Nanog +2160 Reverse	AGGGTCTCAGGTAGCCAAGG	
Nanog +3738 Forward	CCAGTCCCAAACAAAAGCTC	169 bp
Nanog +3906 Reverse	ATCTGCTGGAGGCTGAGGTA	
Nanog +5514 Forward	CTGCTCCGCTCCATAACTTC	97 bp
Nanog +5610 Reverse	GCTTCCAAATTCACCTCCAA	

CHAPTER 3
RESULTS

Generation of an Inducible Fibroblast Growth Factor Receptor 2 Dimerization System

FGFR activation has been shown to be indispensable for PE differentiation. Activation of tyrosine kinase receptors, such as FGF receptors is negatively regulated by tyrosine phosphatases which attenuate growth factor stimulation. We previously showed that addition of sodium vanadate, a protein tyrosine phosphatase inhibitor, to ES cell aggregation cell culture can block the negative feedback loop of protein tyrosine phosphorylation, and is sufficient to induce FGFR mediated primitive endoderm differentiation [51]. Cellular signaling is extremely complex and difficult to dissect. Because sodium vanadate inhibits a broad range of protein tyrosine phosphatases, and conventional ES cell culture uses fetal calf serum that contains a variety of growth factors we sought to develop an inducible system to specifically activate the FGFR2 isotype and downstream signaling using a synthetic small molecule.

Previous studies have demonstrated protein homodimerization can be induced using the human cytoplasmic protein FK506 binding protein (FKBP) with a single phenylalanine to valine substitution at amino acid 36 (F36V) upon addition of a synthetic small molecule dimerizer AP20187[62-64]. This system has been demonstrated to initiate intracellular signaling pathways when expressed in cells as a fusion protein containing drug (F36V FKBP) binding domains linked to intracellular signaling domains. To control fibroblast growth factor signal transduction in ES cells we constructed a pharmacologically inducible FGFR2 receptor by expressing two F36V FKBP domains linked to the intracellular FGFR2 domain which is targeted to the inner face of the plasma membrane through a myristoylation signal, and dimerization is induced by

addition of the dimerizer AP20187 (Figure 3-1 A and B). Additionally, we created an F36V FKBP homodimerization system which lacks FGFR2 intracellular domains to serve as a negative control (Figure 3-1 B). Stable ES cell clones were generated containing control or FGFR2 homodimerization systems and constitutive expression was confirmed by immunocytochemistry staining for the c-terminal hemagglutinin (HA) epitope tag (Figure 3-1C).

FGFR2 Dimerization Effectively Induced Primitive Endoderm Differentiation and *Nanog* Gene Repression

To determine the appropriate dose of AP20187 to activate FGFR2 and its downstream signaling pathways we treated stable ES cells containing the FGFR2 homodimerization system, hereafter called FGFR2 ES cells, with a range of doses from 0.01 to 10 nM. We determined 1 and 10 nM doses were able to robustly phosphorylate Erk1/2 by 90 minutes (Figure 3-1D). Using 10 nM AP20187 we confirmed FGFR2 homodimerization could induce tyrosine phosphorylation of our fusion protein. As expected, we saw an increase in tyrosine phosphorylation in our 78 kilo Dalton (kDa) fusion protein and did not see a band corresponding to wild type FGFR2 receptor at 92 kDa (Figure 3-2A). In addition, we examined phosphorylated substrates p90RSK, Akt, Erk1/2, and S6 ribosomal protein (Figure 3-2B). We found Erk1/2 is rapidly phosphorylated by 15 minutes of AP20187 (10 nM) treatment, and that p90RSK, a downstream effector of Erk1/2, was also phosphorylated, though not as robustly (Figure 3-3B). S6 kinase ribosomal protein is known to be phosphorylated by various mitogen and growth factors, and accordingly, we saw an increase in S6 phosphorylation following FGFR2 homodimerization (Figure 3-2B). Interestingly, FGFR2 homodimerization did not significantly induce Akt phosphorylation (Figure 3-2B).

Next, we examined whether FGFR2 homodimerization can induce primitive endoderm differentiation ES cells harboring a GFP transgene under the control of α-fetoprotein promoter that we previously described[50]. When AFP-GFP FGFR2 ES cells were treated with AP20187 (10nM) for 48 hours, the compact, dome-shaped colony appearance characteristic of undifferentiated ES cells was lost, and the cells adopted a dispersed, differentiated morphology and became GFP positive, indicating these cells differentiate along the PE lineages (Figure 3-3 A). Further, we confirmed differentiation to PE lineage in these cells by reverse transcriptase PCR analysis. We found that *Nanog* mRNA was downregulated in FGFR2 ES cells treated with AP20187 for 48 hours, and these cells additionally express markers of PE including *Gata4*, *Gata6*, and *AFP* (Figure 3-3 B). Interestingly, these cells continue to express the pluripotency associated gene *Oct4* (Figure 3-3 B). Upon examiniation of

FGFR2 Dimerization Rapidly Induces *Nanog* gene downregulation through MEK pathway

We next wanted to examine the kinetics of *Nanog* downregulation comparing two common methods of ES cell differentiation to our system of FGFR2 homodimerization. Both LIF withdrawal and retinoic acid (RA) addition to the media are previously known to downregulate *Nanog* and induce differentiation. We examined *Nanog* gene expression using real-time PCR in ES cells differentiated for 0, 3, 6, or 24 hours. We found that LIF and RA treated cells showed slightly reduced *Nanog* expression by 6 hours and this reduction become more pronounced by 24 hours, when *Nanog* expression was at half the level seen in undifferentiated ES cells (Figure 3-4). FGFR2 homodimerization very rapidly reduced *Nanog* expression over 80% by 6 hours. In addition, both LIF withdrawal and RA addition induce differentiation to a variety of cell

types. The rapid reduction in *Nanog* expression by FGFR2 activation makes this an ideal system to examine the mechanism of *Nanog* downregulation in the context of primitive endoderm specification.

We then examined whether *Nanog* downregulation by FGFR2 dimerization could be prevented by inhibition of FGFR kinase, Mek, or P13K. To do this we utilized *Nanog* β-geo cells and performed x-gal staining to visualize *Nanog* expression in ES cells treated with or without AP20187. In untreated ES cells, we found *Nanog* was heterogeneously expressed, which is consistent with our previously reported observations[60] (Figure 3-5A). In cells treated with AP20187 and the FGFR inhibitor SU5402, we saw an increase and more homogeneous *Nanog* expression pattern, in agreement with the fact that blocking FGFRs can improve ES cell maintenance[65]. In addition, AP20187 treatment with the MEK inhibitor PD98059 partially rescued *Nanog* expression (Figure 3-5A), indicating this pathway is important for *Nanog* downregulation. In contrast, AP20187 induced cells treated with the PI3K inhibitor LY294002 did not prevent *Nanog* downregulation (Figure 3-5A). These effects were not seen in ES cell clones treated with AP20187 which contained the control homodimerization plasmid rather than the FGFR2 kinase domains (Figure 3-5B).

FGFR2 Dimerization Selectively Induced *Nanog* gene downregulation

Next, we analyzed gene expression following a time course of FGFR2 stimulation from 0 to 24 hours. *Nanog* expression is noticeably reduced by 30 minutes, and continues to steadily decrease until transcript expression is reduced over 80% by 6 and 24 hours (Figure 3-6A) and *Gata6* transcript increases between 6 and 24 hours (Figure 3-6D) Interestingly, compared to *Nanog*, expression of key pluripotency transcription

factors *Oct4* and *Sox2* show very different response patterns to FGFR2 stimulation. We found that *Oct4* and *Sox2* remain expressed at a fairly content level through 6 hours of differentiation (Figure 3-6B and C). This indicates that *Nanog* is selectively downregulated among these key pluripotency genes. Interestingly, not all Oct4/Sox2 target genes respond to FGFR2 stimulation like *Nanog*. Upon examination of *Fgf4* and *Utf1*, genes which are both regulated by Oct4 and Sox2 and are expressed in undifferentiated ES cells, we found *Fgf4* is reduced similar to Nanog, but *Utf1* does not respond (Figure 3-6E and F).

In addition to transcripts, we also examined protein levels of Nanog, Oct4, Sox2, and phosphorylated Erk1/2 (Figure 3-3 C) over a time course of AP20187 (10 nM) treatment. As expected, we found homodimerization of FGFR2 ES cells induced Erk1/2 phosphorylation (Figure 3-3C). We found that Oct4 protein is maintained through 48 hours of homodimerization, which is consistent with our *Oct4* mRNA PCR data, and additionally, we found that Sox2 protein is also maintained (Figure 3-3C). Notably, we found Nanog protein is downregulated by 6 hours, which in conjunction with the *Nanog* mRNA data, indicates *Nanog* is downregulated following FGFR2 homodimerization (Figure 3-3C).

FGFR2 Dimerization Induced Transcriptional Repression of *Nanog*

The rapid reduction in *Nanog* mRNA and protein following FGFR2 stimulation promoted us to examine whether *Nanog* is downregulated at the transcription or post-transcription level. To do this, we examined *Nanog* pre- spliced mRNA (Pre-mRNA) by real-time PCR using intron and exon sense and antisense primers, respectively. As a control, we also examined expression of *Oct4* pre-mRNA because we did not see a decrease in *Oct4* mRNA previously. We found FGFR2 stimulation induced a rapid

downregulation in *Nanog* pre-mRNA which paralleled what we saw with *Nanog* mRNA, indicating *Nanog* is not longer highly transcribed (Figure 3-7A). In contrast, and as we expected, *Oct4* pre-mRNA does not decrease significantly over the time course of FGFR2 stimulation (Figure 3-7B). These data indicate that *Nanog* is transcriptionally downregulated following FGFR2 dimerization.

Histone modifications including acetylation, phosphorylation, methylation, and ubiquitination, can play important roles in gene regulation[66] . Chromatin immunoprecipitation (ChIP) is a powerful tool to study the localization of various histone modifications. Here, we chose to map a number of histone 3 (H3) methylation modifications across the *Nanog* gene locus to better understand how chromatin may play a role in *Nanog* repression following FGFR2 stimulation. H3 methylation at lysines 4, 36, and 79 is generally associated with active/permissive chromatin, while methylation of lysine residues 9 and 27 is associated with repressed chromatin. We examined methylation marks on histone H3 including lysine 4 trimethylation (H3K4me3), lysine 9 trimethylation (H3K9me3), lysine 27 trimethylation (H3K27me3), and lysine 36 trimethylation (H3K36me3). H3K4me3 is reported around the start sites of active genes, while H3K36me3 is reported to increase through the gene body towards the 3' end of active genes representing active transcriptional elongation[67]. H3K9me3 and H3K27me3 are typically enriched in the promoter and around the transcription start sites of repressed genes[67].

Here we mapped the distribution of H3 K4me3, K36me3, K9me3, and K27me3 across the *Nanog* locus at high resolution. Because our ChIP sonication conditions shear chromatin to an average of length of 500 bp, with a range between 200 and 1,000

bp, we designed six primer sets spaced an average of 1,500 bp apart to visualize enrichment of various proteins. We examine protein binding of histone modifications and RNA Polymerase II (RNA Pol II) enrichment at the *Nanog* locus is FGFR2 ES cells stimulated with AP20187 (10 nM) for 0,6, or 24 hours, and demonstrate gradual changes within the locus during *Nanog* downregulation following FGFR2 homodimerization.

In undifferentiated ES cells, we found the H3K36me3 modification is enriched towards the 3' end of *Nanog* coding region (Figure 3-8B). This modification is seen at a very low level of enrichment in the promoter region and around the transcription start site, slightly increased through intron 1, and is strongly increased by exons 2 and 4. This distribution is consistent with previous reports of K36me3 in active chromatin, and indicates the *Nanog* gene is actively transcribed and elongation of the transcript occurs. After 6 hours of differentiation induced by AP20187 (10 nM) we see a comparable level of K36me3 in the promoter, transcription start site, and intron 1, to undifferentiated ES cells. In contrast, we see a significant decrease in enrichment by exon 2. This pattern suggests that transcriptional elongation is significantly decreased in these early differentiating cells. By 24 hours of differentiation, this pattern is more pronounced, with a near total decrease in the K36me3 modification throughout the *Nanog* locus. Loss of theK36me3 modification during differentiation indicates the *Nanog* transcript is no longer actively elongating.

Next, we examined H3K4me3 mark of active chromatin. We found this modification is enriched in undifferentiating ES cells near to the transcription start site and intron 1 and enrichment tapers off towards the 5' promoter end of the locus, and

also towards the 3' coding region of the gene (Figure 3-8C). FGFR2 ES cells treated with AP20187 for 6 hours display a marked increase in enrichment of H3K4me3 in the 5' promoter region, around the transcription start site, and into the first intron. This broadening enrichment is largely decreased in FGFR2 ES cells treated with AP20187 (10 nM) for 24 hours. In these cells, we see enrichment is similar to undifferentiated cells, where there is an increase in H3K4me3 association around the transcription start site and intron1 with a decrease to the 3' end. Notably, there still appears to be increased enrichment in the promoter region of the gene. While our PCR data indicates *Nanog* mRNA is downregulated, the persistent enrichment of the histone modification H3K4me3 may indicate this locus retains an open chromatin conformation in the early stages of differentiation, and that the *Nanog* gene chromatin takes more time to become closed.

We examined enrichment of RNA pol II using an antibody which specifically recognizes the phosphorylated c-terminal domain serine 5 version of the enzyme, which is indicative of RNA Pol II initiation. Here we found undifferentiated ES cells display enrichment for RNA Pol II around the transcription start site (Figure 3-9B). This binding pattern was increased in ES cells stimulated with AP20187 (10 nM) for 6 hours. Binding of RNA Pol II is reduced to a very low level in ES cells stimulated with AP20187 for 24 hours. This indicates *Nanog* is no longer actively transcribed by 24 hours, but the increase seen at 6 hours was unexpected. In addition, we also examined binding of the transcriptional co-activator p300. We found p300 is slightly enriched at the transcription start site in undifferentiated ES cells and that this pattern is not significantly changed following 6 or 24 hours of FGFR2 homodimerization induced by AP20187 (10 nM)

(Figure 3-9C). It is possible that this co-activator protein dissociates from the locus at a later time.

We also examined histone modifications H3K9me3 and H3K27me3, which are associated with repressed chromatin (Figure 3-10B and C). We found undifferentiated ES cells displayed very low enrichment of H3K9me3 over the entire gene locus, as expected. In 6 and 24 hour FGFR2 stimulated cells, however, we saw very little increase in this modification. In addition, we saw a similar pattern of H3K27me3 at the *Nanog* locus. Again, we found that undifferentiated ES cells show very little enrichment of this histone modification, though there is a small increase seen towards the 3' end of the gene in exons 2 and 4. Notably, we did not see a significant increase in this histone modification in ES cells treated with AP20187 (10 nM) for 6 or 24 hours. This indicates that these repressive histone marks are likely acquired at a later time in the differentiation process.

The Proximal Promoter Region Is Sufficient for FGFR2 Dimerization Induced *Nanog* Downregulation

To determine the region of the *Nanog* promoter responsive to FGFR2 stimulation, we constructed reporter vectors containing 2,300, 330, or 150 base pair (bp) length promoter regions of *Nanog* which drive expression of β-galactosidase and confer neomycin resistance (Figure 3-11 A). Previously, Oct4 and Sox2 binding sites located between -180 and -165 upstream of the *Nanog* transcription start site have been shown to be essential for transcriptional activation[46, 47]. Originally, we planned to integrate these reporters into the active HPRT locus using a knock-in approach. To accomplish this we constructed our reporters to contain 5' and 3' homologous arms to the HPRT locus. In the end, targeted integration failed and we randomly integrated the reporters

to produce stable transgenic ES cells containing 2,300, 330, or 150 bp reporters using G418 selection (Figure 3-11A). Each of the transgenic cell lines were stimulated by FGFR2 dimerization and the kinetics of β-geo and endogenous *Nanog* transcripts were compared by real-time PCR of mRNA. We found that both the 2,300 and 330 bp ES cells displayed similar β-geo and endogenous *Nanog* transcript kinetics in cells treated for 3 hours with AP20187(10 nM) (Figure 3-11B and C). In contrast, the 150 bp reporter ES cells did not show a decrease in β-geo transcript (Figure 3-11D), indicating the FGFR2 response element mediating *Nanog* downregulation is located between –330 and –150 in the proximal promoter region of *Nanog*.

These results were obtained using random integration of reporters, and there are various limitation associated with this method. One of these is variable transgene expression due to integration of different copy numbers at genomic sites. In addition, it is possible for the transgene to integrate next to a repressor or enhancer, and the transgene will be subject to the regulation of another gene. To combat these problems and to further define the response element required for FGFR2 mediated *Nanog* downregulation, we constructed luciferase reporter constructs containing comparable 2,300, 330, and 150 bp promoter regions. We constructed these reporters by PCR amplification of genomic DNA, digestion, and ligation into pGL2-Basic vector lacking eukaryotic promoter and enhancer sequences, so expression of firefly luciferase activity would depend on *Nanog* promoter fragments inserted upstream of the reporter gene. FGFR2 ES cells were transiently transfected with one reporter construct and 48 hours later were treated with AP20187 (10 nM) for 6 hours. Firefly luciferase activity was normalized to *Renilla* luciferase to control for transfection efficiency. In unstimulated ES

cells, we found the 150 bp promoter displayed a low level of firefly luciferase activity, which is consistent with previous reports that indicate the Oct4 and Sox2 consensus sequence located further upstream of -150 bp is important for robust transcriptional activation[46, 47] (Figure 3-12A). We found the 330 and 2,300 bp reporters expressed higher levels of firefly luciferase, where the 2,300 bp reporter was highest, consistent with reports that additional transcriptional activators bind upstream of the Oct4 and Sox2 consensus sites (Figure 3-12A). We found that cells treated with AP20187 for 6 hours did not show a significant decrease in luciferase activity, indicating these transiently transfected reporters do not respond to FGFR2 stimulation (Figure 3-12A).

We hypothesized that stable integration may be required for mediating FGFR2 induced *Nanog* downregulation. To examine this, we stably integrated the 330 bp firefly luciferase reporter into FGFR2 ES cells containing the stably integrated 330 bp *Nanog* β–geo reporter. Cells were treated with 0 or 6 hours of AP20187 (10 nM) and were harvested to examine β-geo, endogenous *Nanog*, or firefly luciferase transcript using real-time PCR. In contrast to our expectations, we found the luciferase transcript did not respond to FGFR2 stimulation while the Nanog β-geo and endogenous *Nanog* transcripts did (Figure 3-12B). This result led us to hypothesize that the homologous arms in the β-geo constructs may behave as an insulator to protect the transgene from nearby regulatory elements.

To examine this, we altered the original 330 bp *Nanog* β-geo construct to remove the homologous HPRT arms. Next, we stably integrated the reporter into FGFR2 ES cells and treated cells with 0 or 6 hours of AP20187 (10 nM). We examined β-geo and endogenous *Nanog* transcripts using real-time PCR. Interestingly, we found treatment

decreased endogenous *Nanog*, but not the β-geo transcript, which is consistent with the idea that the homologous arms may have been acting as an insulator (Figure 3-12C). We next decided to generate reporter vectors flanked by the well characterized chicken β–globin HS4 insulator.

The HS4 core insulator from the chicken β-globin locus is known to act as an insulator. Typically, a transgene is flanked by two copies of the HS4 core to shield the transgene from chromosomal position effects after stable integration. We planned to modify the *Nanog* promoters driving expression of the luciferase reporter which we previously used in transient transfection assays, by flanking the transgene with two copies of the HS4 core insulator. We were only able to successfully clone the HS4 copies on the 5' end of our transgene, though because transgenes are usually inserted as multiple copies in a single location; it is possible to insert insulator elements on only one side of the transgene. To follow this strategy, we removed any unnecessary vector backbone, and transfected FGFR2 ES cells with the 330 bp insulated *Nanog* luciferase reporters or a shorter 190bp reporter (Figure 3-13C). These cells were also co-transfected with a vector conferring puromycin resistance so that we could generate stable clones after drug selection.

Four individual transgenic cell lines clones containing either the 330 bp or 190 bp reporters were stimulated by FGFR2 dimerization and the kinetics of luciferase and endogenous *Nanog* transcript mRNA were compared by real-time PCR. We found that endogenous *Nanog* and luciferase transcripts displayed similar kinetics in both the 330 bp and 190 bp reporters, where both luciferase and endogenous *Nanog* mRNA were rapidly downregulated after 6 and 24 hours of FGFR2 stimulation by AP20187

treatment (Figure 3-14A and B). These results confirmed our previous work with the *Nanog* β-geo reporters flanked by HPRT arms, and further indicated the 190 bp *Nanog* promoter is sufficient for FGFR2 mediated *Nanog* downregulation. Interestingly, this reporter promoter ends just 5' to the Oct4 and Sox2 consensus binding sites.

To examine whether the Oct4/Sox2 consensus sequences are important for FGFR2 mediated *Nanog* downregulation, we constructed additional insulated luciferase reporter vectors containing only the Oct4/Sox2 consensus binding sequence from the *Nanog* promoter (-185 to -160 bp upstream of the transcription start site) followed by a minimal thymidine kinase (TK) promoter (-155 to +50) which maintains the distance between the binding elements and the transcription start site (Figure 3-14C). In addition, we constructed a TK promoter (-190 to +50) which also maintains this distance but lacks any *Nanog* sequence to serve as a negative control reporter. After generating stable reporter clones we stimulated FGFR2 dimerization with AP20187 to induce *Nanog* downregulation and PE differentiation. We examined the kinetics of luciferase and endogenous *Nanog* transcript mRNA in the Oct4/Sox2 TK reporter by real-time PCR for four individual clones, and found that endogenous *Nanog* mRNA was rapidly downregulated after 6 and 24 hours of FGFR2 stimulation by AP20187 treatment (Figure 3-14C). In addition, luciferase transcripts also decreased following 6 and 24 hours of treatment, thought the kinetics appear slightly slower than endogenous *Nanog* at the 6 hour time point (Figure 3-14C). However, by 24 hours of AP20187 treatment, these transcripts were downregulated to comparable levels, indicating the –190 to -160 bp region of the Nanog *promoter* contains an FGFR2 responsive element that mediates *Nanog* downregulation. The control 190bp TK reporter clones displayed a

rapid decrease in *Nanog* mRNA following 6 and 24 hours of FGFR2 dimerization, however, luciferase transcripts did not similarly decrease by 6 or 24 hours (Figure 3-14D). This indicates the reduction in promoter activity is not a general phenomenon as it was not seen in the TK reporter lacking *Nanog* promoter elements.

FGFR2-Mediated Nanog Downregulation Did Not accompany with Oct4/Sox2 Dissociation from the Proximal Promoter Region

Because Oct4 and Sox2 are known to bind to eachother and to this region of the *Nanog* promoter, we hypothesized one of both of these proteins may dissociate from the *Nanog* promoter to mediate downregulation following FGFR2 stimulation. We examined Oct4 and Sox2 binding to the proximal promoter to determine whether enrichment of one or both factors is altered by FGFR2 stimulation. Using ChIP, we found that Oct4 and Sox2 are both enriched around the Oct4/Sox2 binding site in undifferentiated ES cells, as previously reported, and found that 6 hours of FGFR2 stimulation does not significantly reduce binding, though after 24 hours of FGFR2 stimulation there does appear to be an overall decrease in Oct4 enrichment (Figure 3-15B). The persistence of binding at 6 hours, at a time when *Nanog* transcript is reduced more than 80% suggests that Oct4/Sox2 dissociation from the proximal promoter region is not a cause for FGFR2-mediated *Nanog* downregulation.

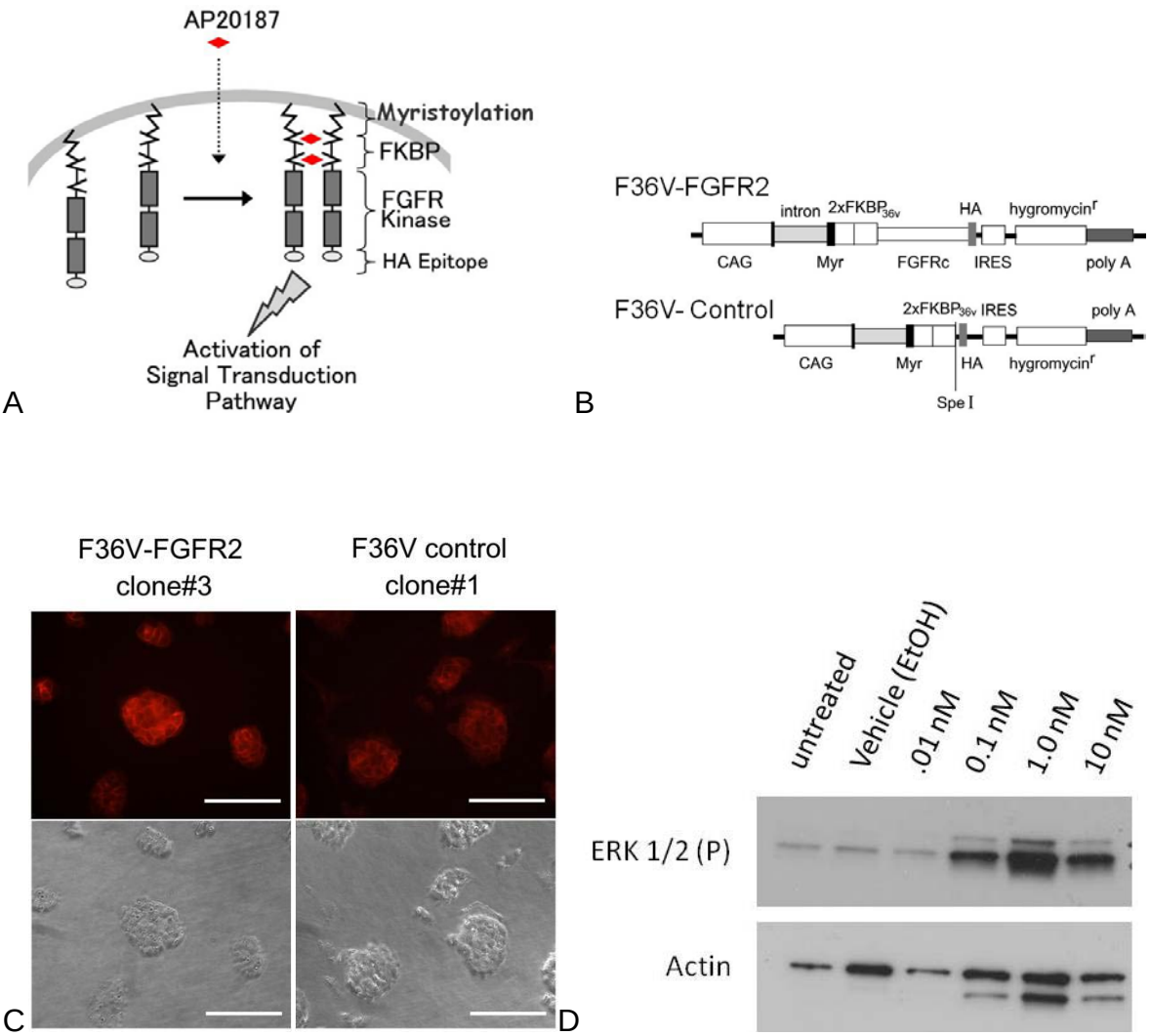

Figure 3-1. Inducible FGFR2 homodimerization system. A) Schematic representation of the FGFR2 activation system. AP20187 synthetic ligand binds to two FKBP domains located on the inner face of the plasma membrane. Ligand binding induces fusion protein dimerization and activates FGFR2 kinase domains to initiate downstream signal transduction. B) Plasmid constructs for generation of FGFR2 and control FKBP activation systems. C) Immunocytochemistry staining of ES cell clones that stably express FGFR2 or control FKBP activation systems using anti-HA antibody. Scale bar: 100 μm. D) Immunoblotting for Erk1/2 phosphorylation after 90 minutes of AP20187 treatment at a range of dimerizer concentrations from .01 to 10 nM.

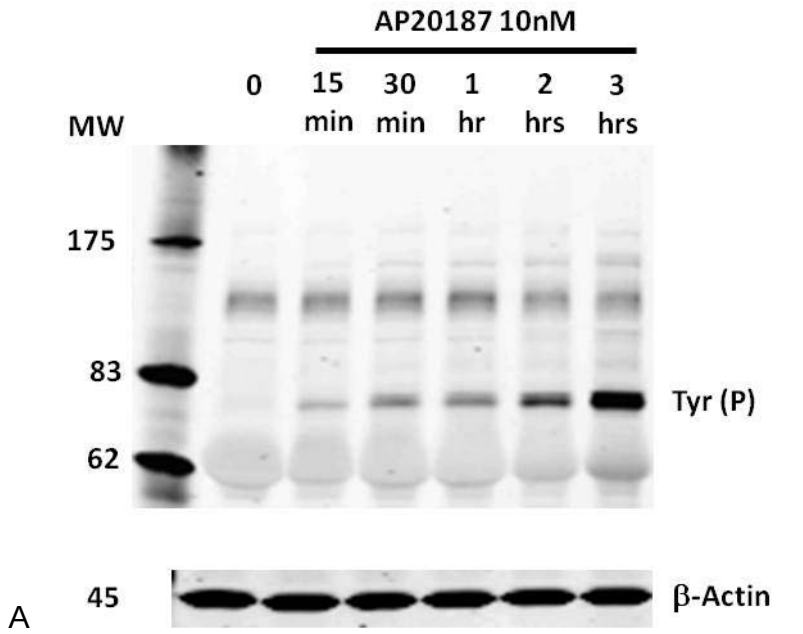

A

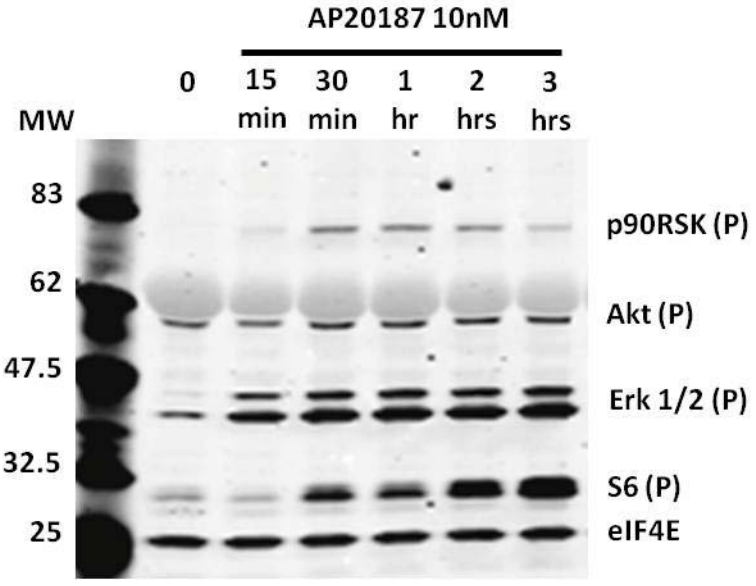

B

Figure 3-2. FGFR2 homodimerization induces tyrosine phosphorylation and Erk1/2 phosphorylation. ES cells stably expressing FGFR2 homodimerization system were treated with or without AP20187 (10 nM) over a timecourse (15 minutes to 3 hours). Immunoblotting was performed using A) anti-phosphotyrosine and β-actin control antibodies or B) anti-phospho-p90RSK, Akt, Erk1/2, S6, and control eIF4E antibodies.

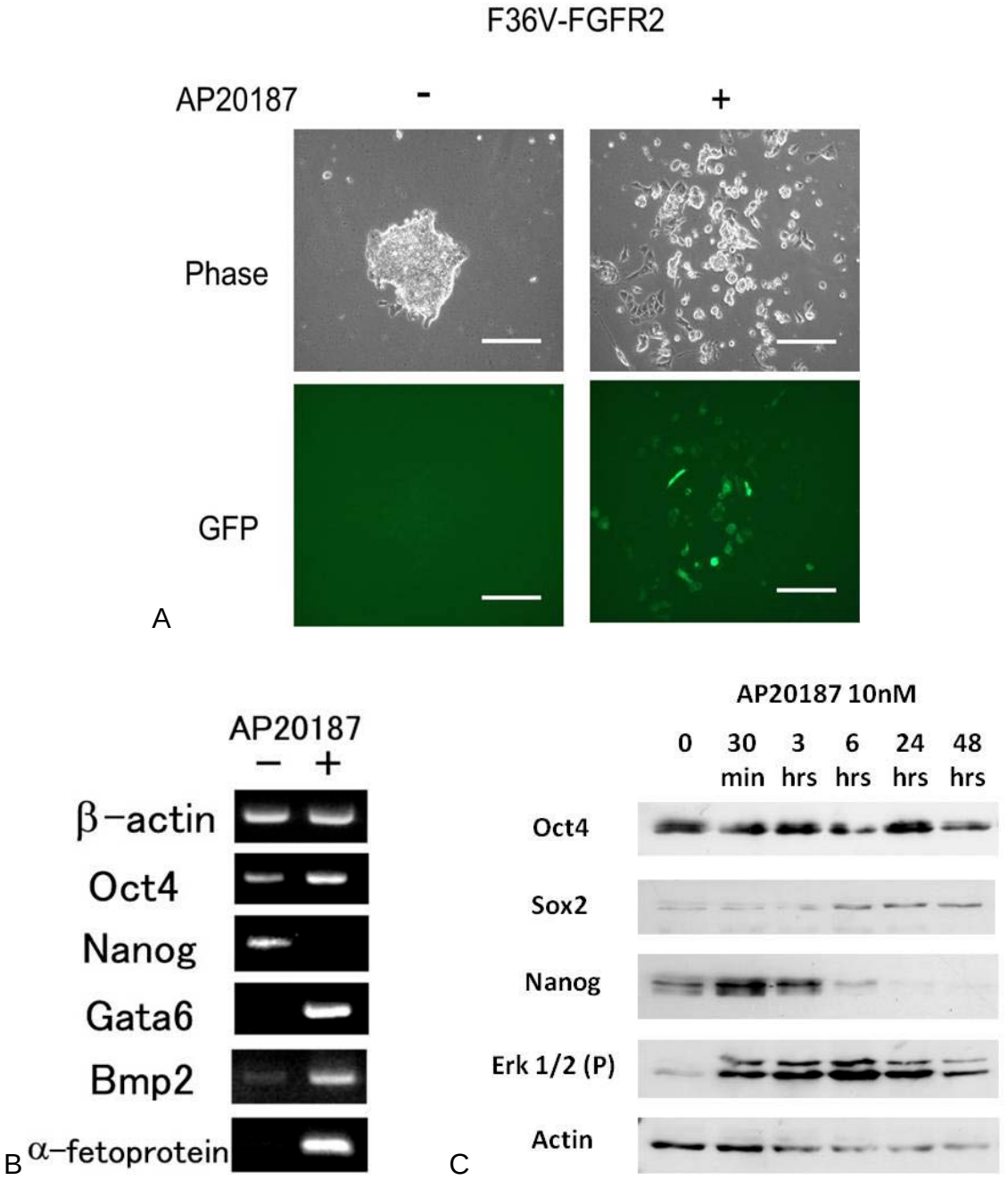

Figure 3-3. FGFR2 homodimerization induces primitive endoderm differentiation and *Nanog* downregulation. A) Afp-GFP ES cells stably expressing FGFR2 homodimerization system were treated with or without AP20187 (10 nM) for 48 hours. Images of representative colonies are shown using phase contrast (upper panels) or GFP filter (lower panels) microscopy. Scale bars: 200 μm. B) RT-PCR analysis of gene expression in FGFR2 ES cells treated with or without AP20187 (10 nM) for 48 hours. C) Immunoblotting was performed over an AP20187 (10 nM) treatment time course (0-48 hours).

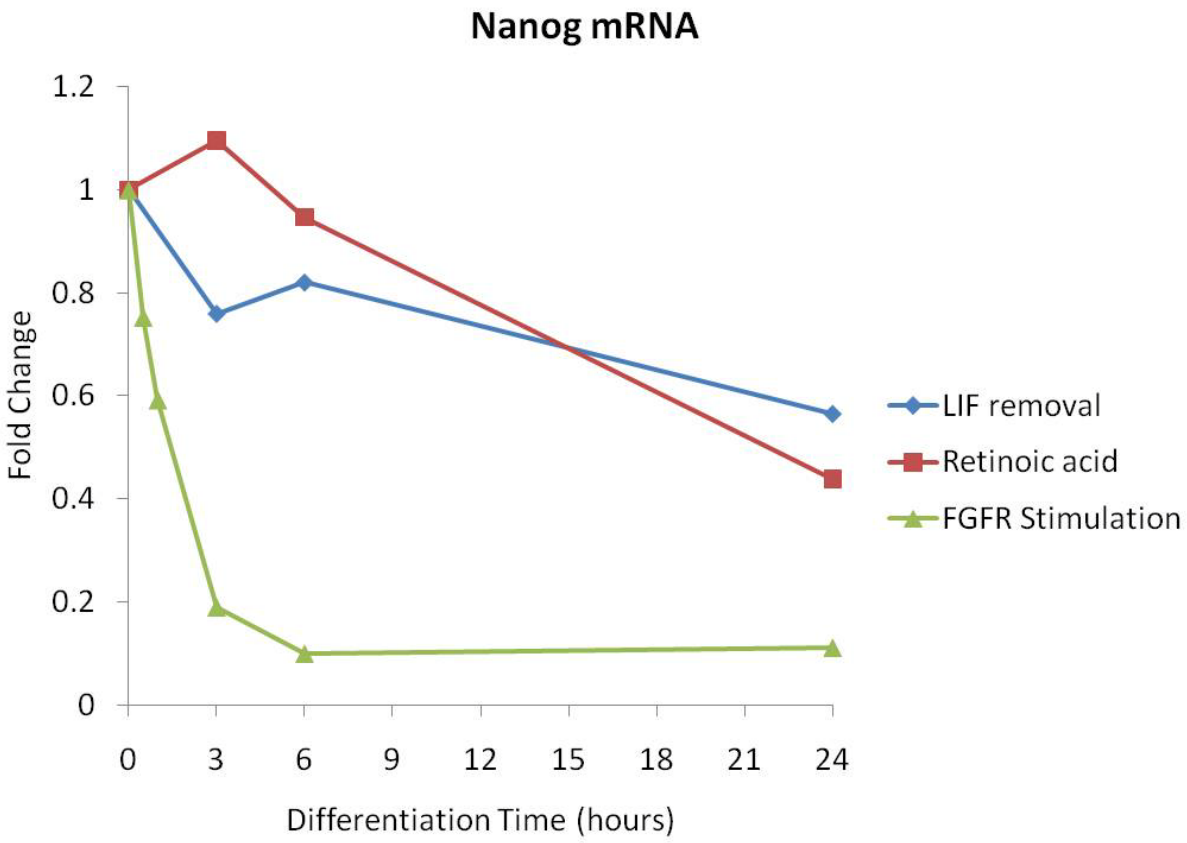

Figure 3-4. FGFR2 homodimerization rapidly reduces *Nanog* expression. Real-time PCR analysis of *Nanog* mRNA in ES cells induced to differentiate using LIF removal, retinoic acid treatment (1 μM), or FGFR2 homodimerization using AP20187 (10 nM). Cells were harvested over the differentiation time course (0-24 hours). Average mRNA value relative to β-actin is expressed as fold change over time, where 0 hrs is set to a value of 1.

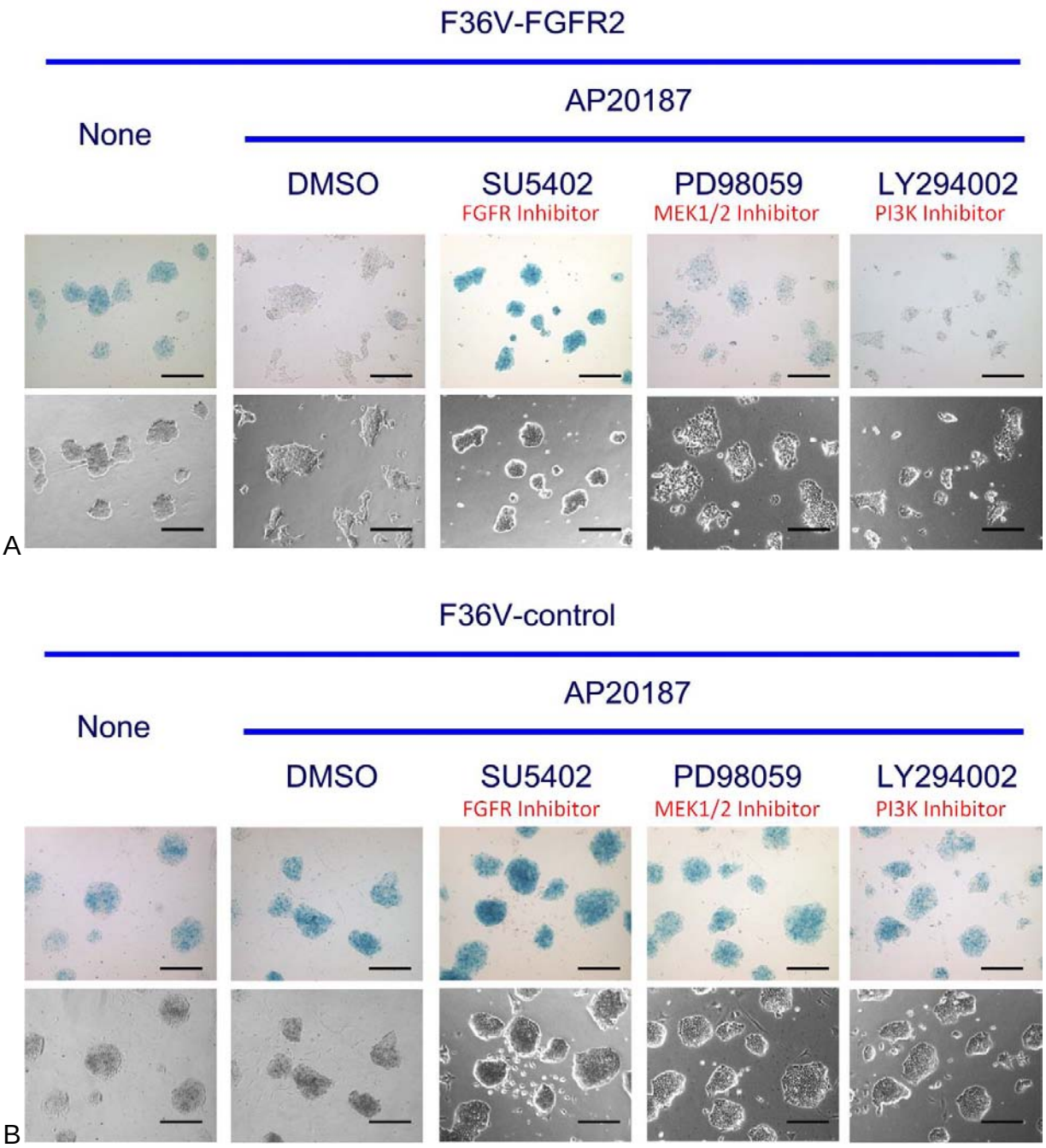

Figure 3-5. FGFR2 homodimerization induced *Nanog* downregulation can be prevented by FGFR or Mek1/2 inhibitors. A) *Nanog* β-geo ES cells containing F36V FGFR2 or B) F36V control construct were treated with AP20187 (10 nM) for 48 hours and either vehicle control (DMSO), FGFR inhibitor (SU5402), Mek1/2 inhibitor (PD98059), or PI3K inhibitor (Lys94002) and stained with x-gal to examine *Nanog* expression. Scale bar: 200 μm.

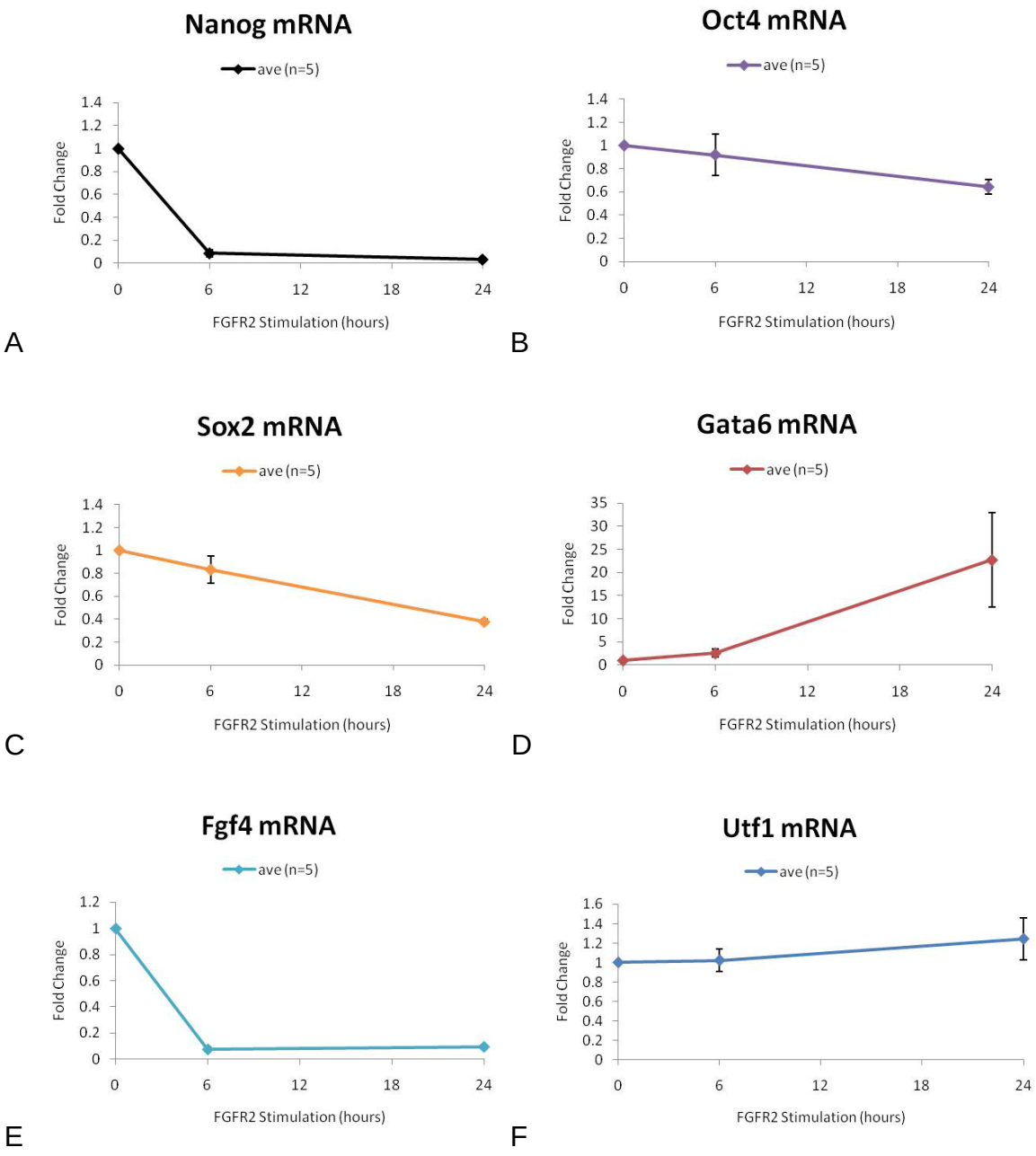

Figure 3-6. FGFR2 homodimerization selectively reduces *Nanog* expression. Real-time PCR analysis of key pluripotency genes A) *Nanog* mRNA, B) *Oct4* mRNA, C) *Sox2* mRNA, D) primitive endoderm marker *Gata6* mRNA, or Oct4/Sox2 target genes E) *Fgf4*, and F) *Utf1*. ES cells were harvested after 0, 6, or 24 hours of treatment with AP20187 (10 nM). Average mRNA value of 5 experiments relative to *β-actin* is expressed as fold change over time, where 0 hrs is set to a value of 1. Error bars indicate standard deviation.

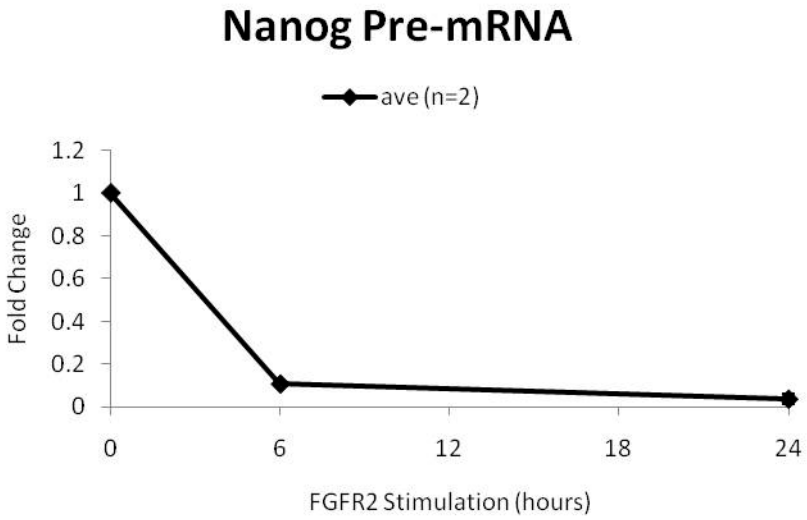

A

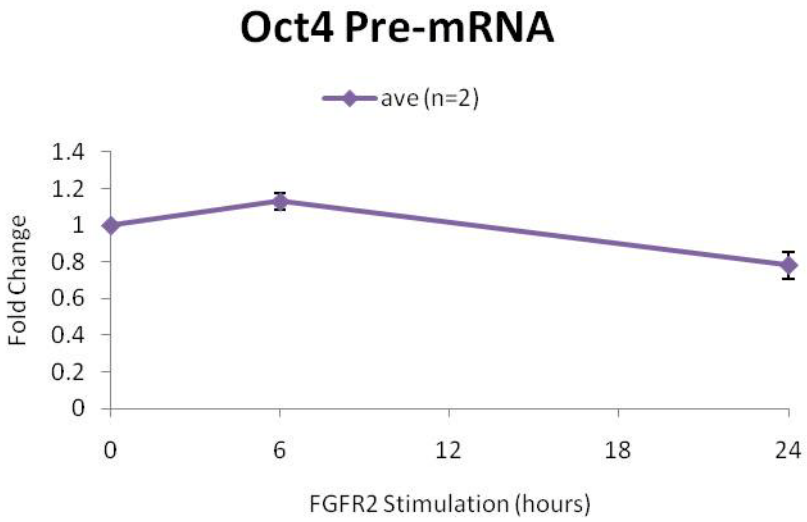

B

Figure 3-7. *Nanog* downregulation by FGFR2 homodimerization occurs at the transcriptional level. Real-time PCR analysis of (A) *Nanog* or (B) *Oct4* pre-spliced mRNA. ES cells were harvested after 0, 6, or 24 hours of treatment with AP20187 (10 nM). Average mRNA value of 2 experiments relative to *β-actin* is expressed as fold change over time, where 0 hrs is set to a value of 1. Error bars indicate standard deviation.

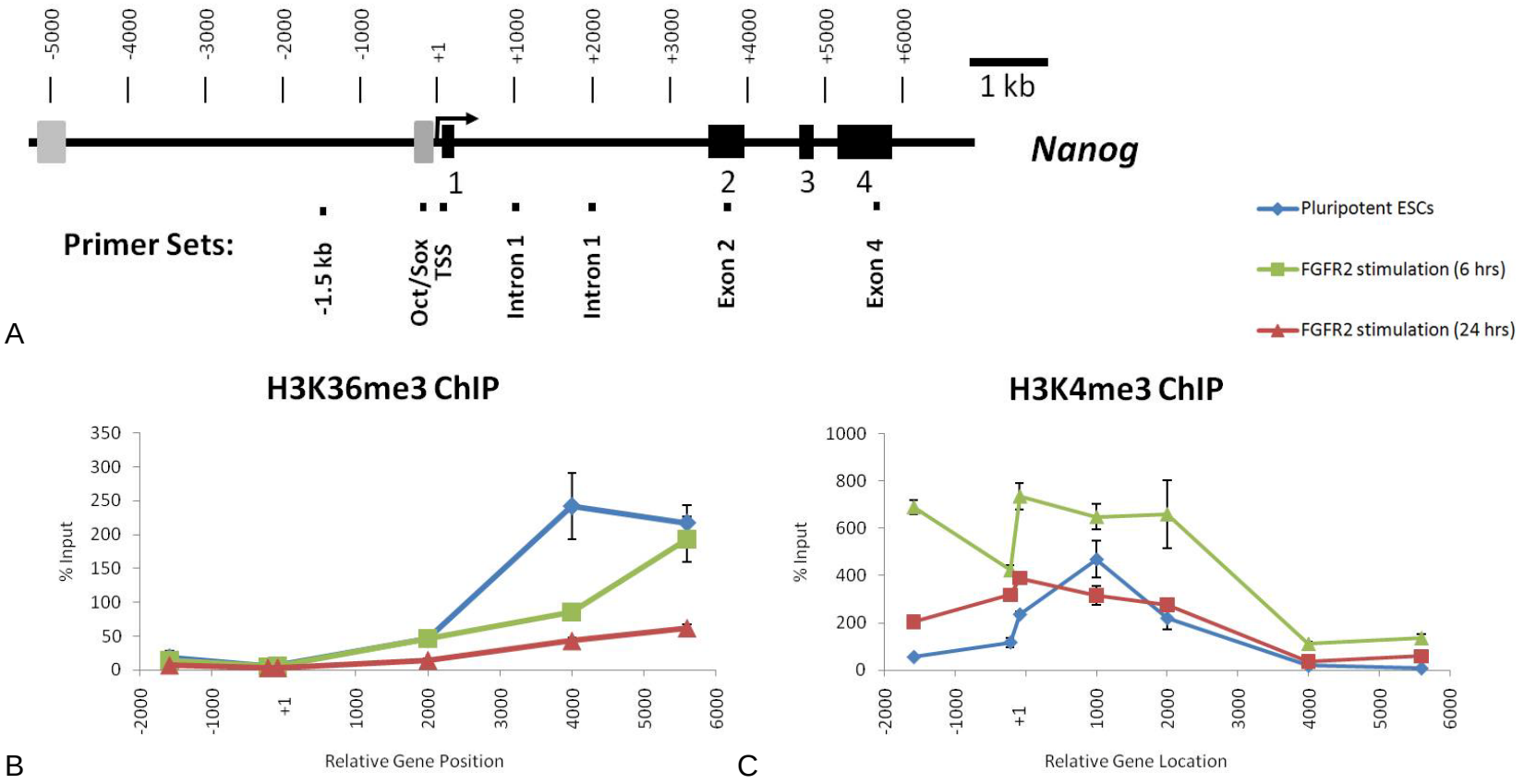

Figure 3-8. FGFR2 homodimerization reduces H3K36me3 enrichment at the 3' end of the coding region and transiently increases and broadens H3K4me3 enrichment around the transcription start site at the *Nanog* locus. A) Schematic of *Nanog* locus with location of real-time PCR primers for analysis of chromatin immunoprecipitation assays. B) Real-time PCR analysis of enrichment of histone H3 lysine 36 trimethylation and histone H3 lysine 4 trimethylation at the *Nanog* locus in ES cells harvested after 0, 6, or 24 hours of treatment with AP20187 (10 nM). Enrichment is expressed as % input. Samples were run in triplicate for each primer and the average % input is plotted. Error bars indicate standard deviation.

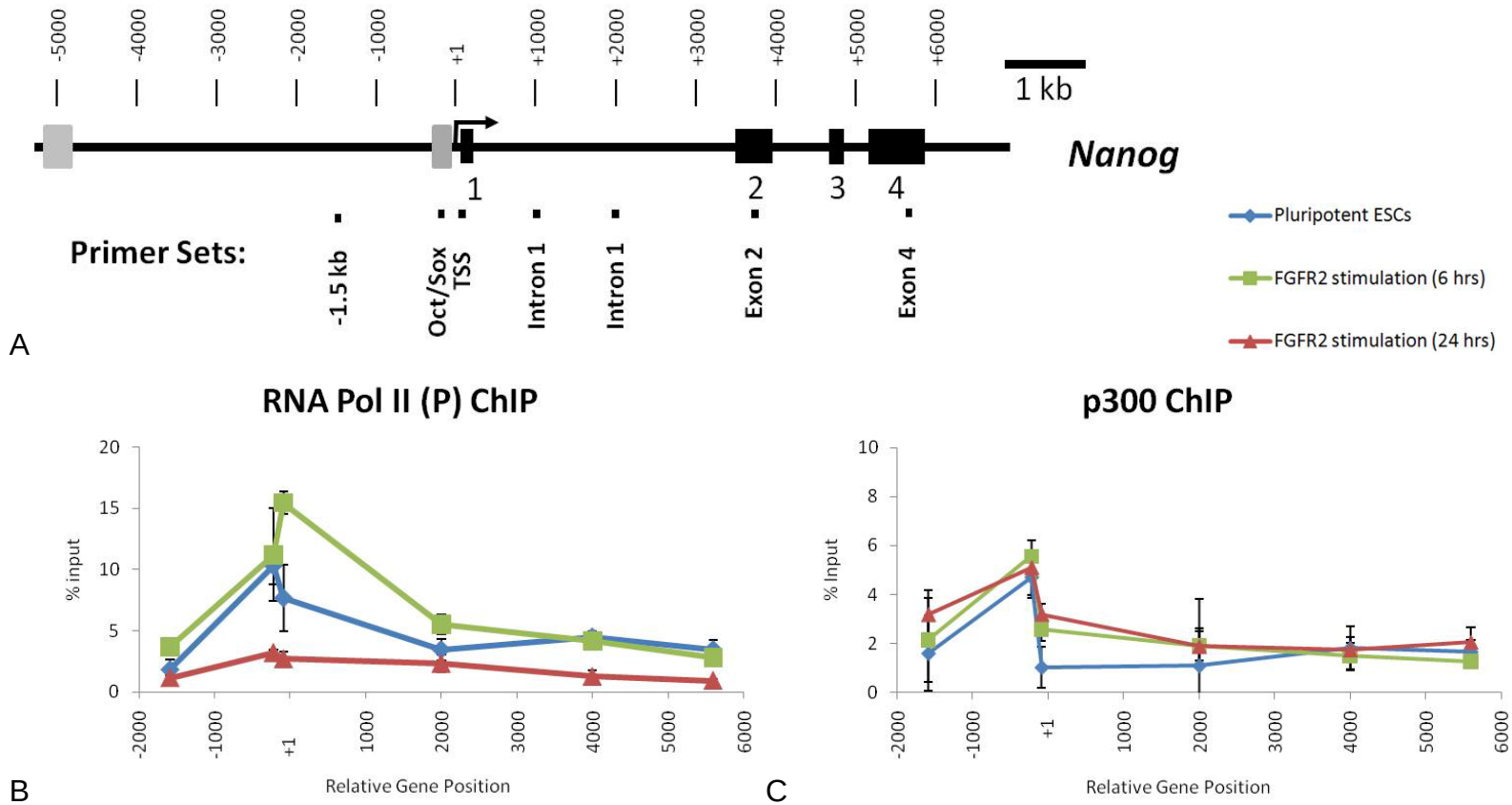

Figure 3-9. FGFR2 homodimerization transiently increases RNA Polymerase II enrichment around the transcription start site at the *Nanog* locus without significant reduction in p300 co-activator enrichment. A) Schematic of *Nanog* locus with location of real-time PCR primers for analysis of chromatin immunoprecipitation assays. B) Real-time PCR analysis of enrichment of histone serine 5 phosphorylated RNA Polymerase II and p300 co-activator at the *Nanog* locus in ES cells harvested after 0, 6, or 24 hours of treatment with AP20187 (10 nM). Enrichment is expressed as % input. Samples were run in triplicate for each primer and the average % input is plotted. Error bars indicate standard deviation.

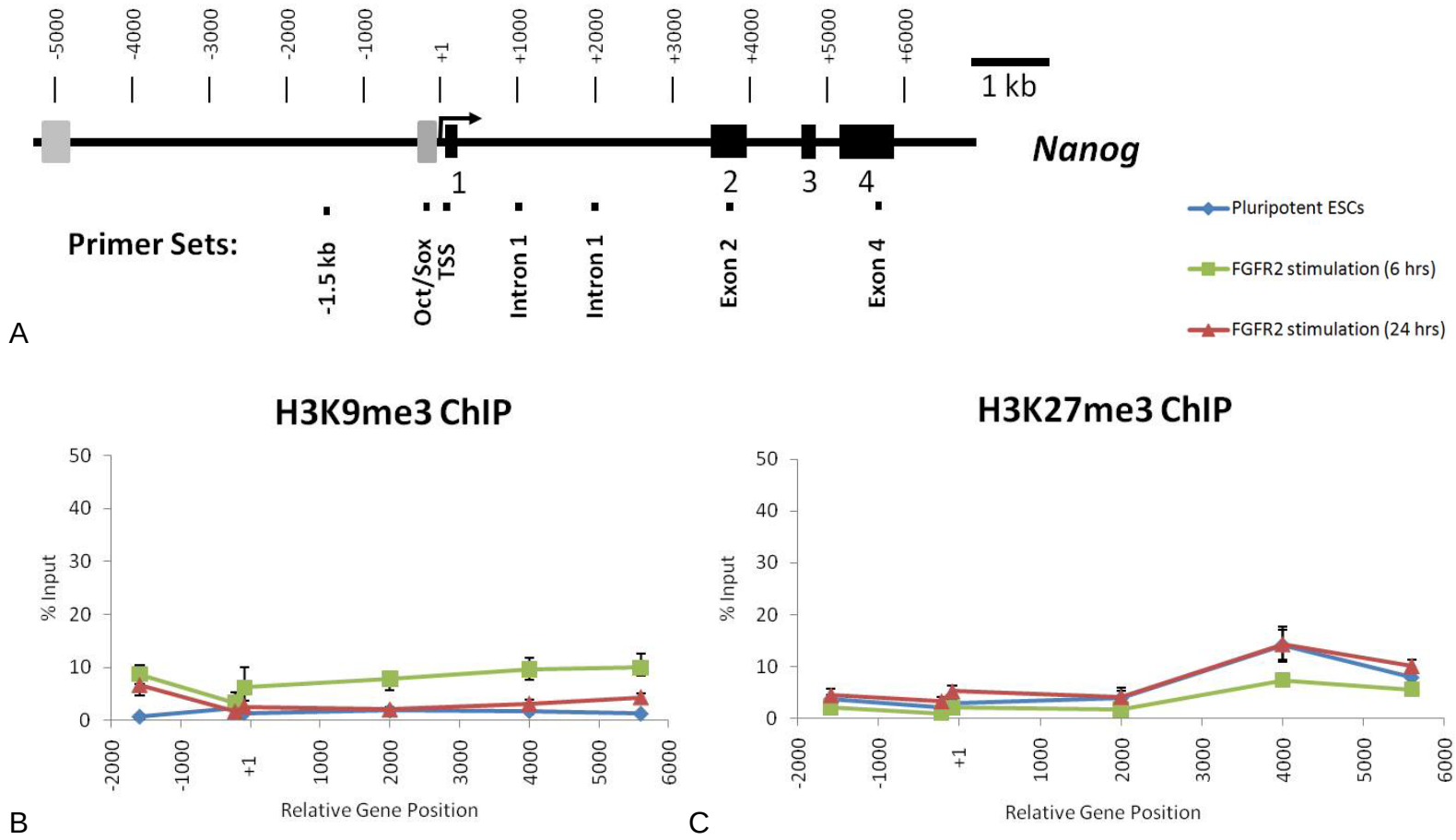

Figure 3-10. FGFR2 homodimerization does not greatly increase histone modifications associated with repressed chromatin. A) Schematic of *Nanog* locus with location of real-time PCR primers for analysis of chromatin immunoprecipitation assays. B) Real-time PCR analysis of enrichment of histone H3 lysine 9 trimethylation and histone H3 lysine 27 trimethylation at the *Nanog* locus in ES cells harvested after 0, 6, or 24 hours of treatment with AP20187 (10 nM). Enrichment is expressed as % input. Samples were run in triplicate for each primer and the average % input is plotted. Error bars indicate standard deviation.

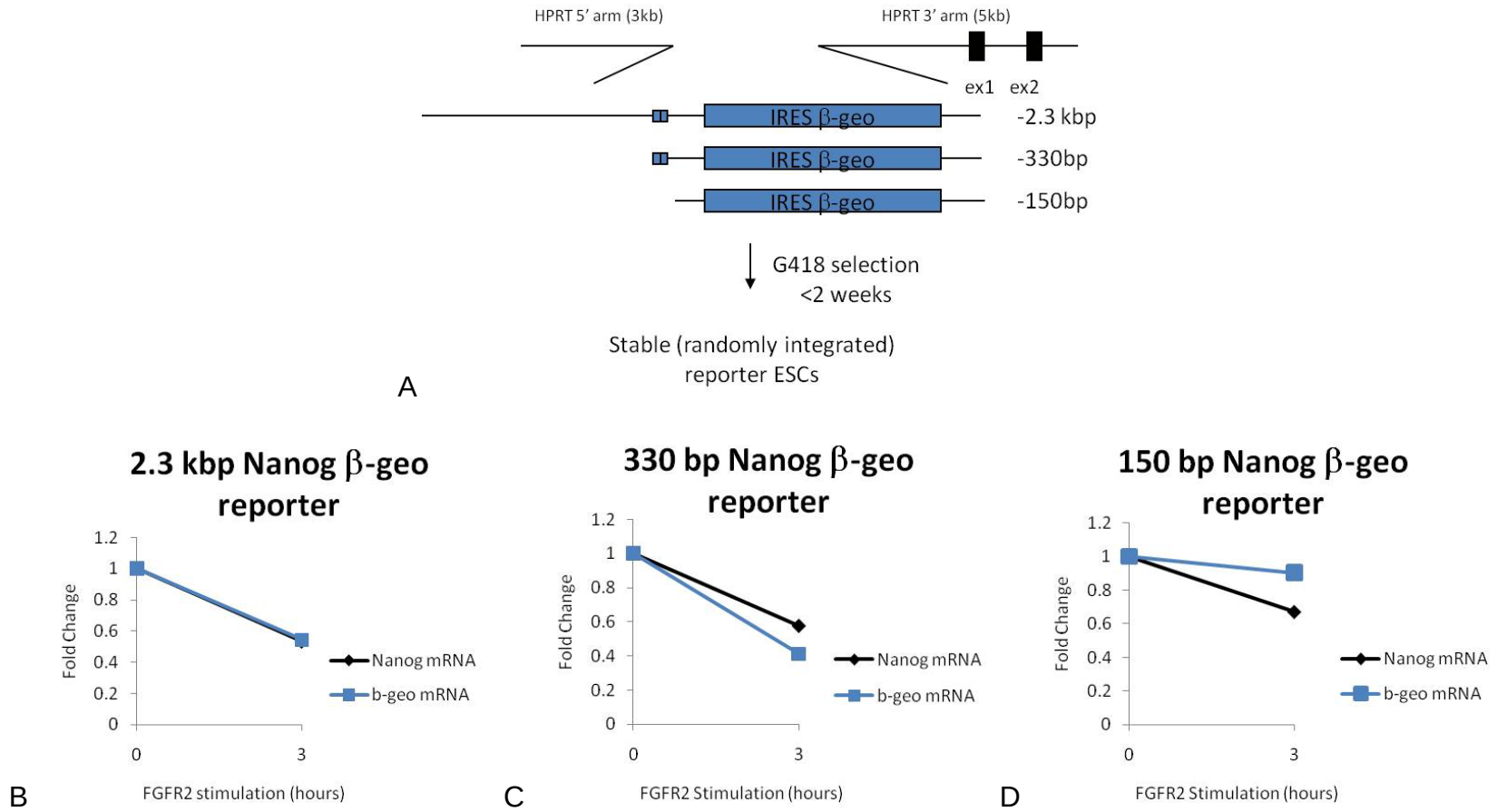

Figure 3-11. Integrated *Nanog* β-geo reporters indicate the 330 bp proximal promoter is sufficient for FGFR2 induced *Nanog* downregulation. A) Schematic of *Nanog* β-geo reporter plasmids. FGFR2 R1 ES cells containing a B) 2,300bp, C) 330 bp, or D) 150 bp β-geo reporter were harvested after 0 and 3 hours of treatment with AP20187 (10 nM). Real-time PCR was performed to examine expression of *Nanog* or *β-geo* transcripts. Average mRNA value relative to *β-actin* is expressed as fold change over time, where 0 hrs is set to a value of 1.

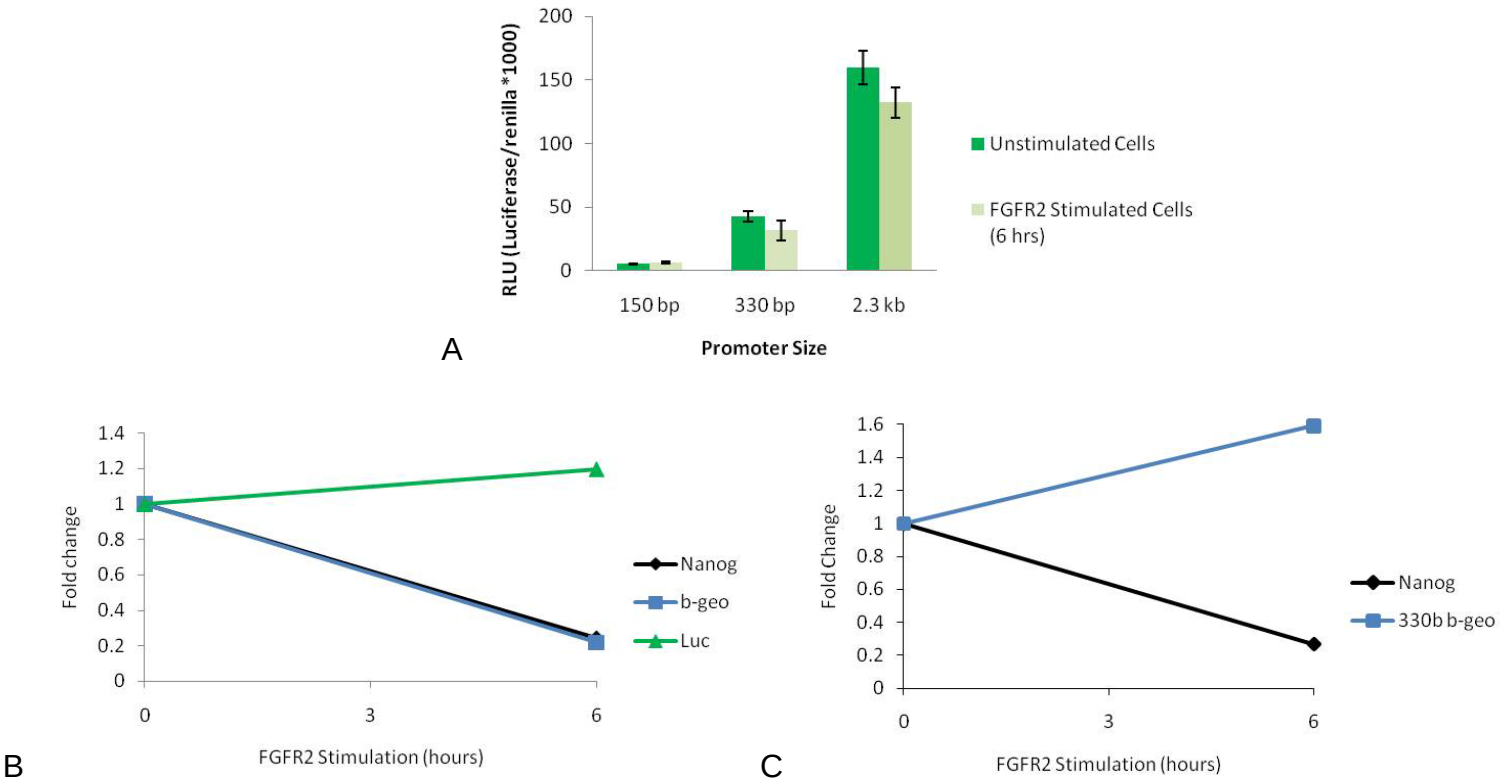

Figure 3-12. Transiently or stably transfected *Nanog* reporters lacking HPRT arms do not respond to FGFR2 homodimerization. A) FGFR2 R1 ES cells were transiently transfected with 2,300, 330, or 150 bp luciferase reporter plasmids and cells were harvested after 0 and 6 hours of treatment with AP20187 (10 nM). Firefly and Renilla luciferase was measured. Relative luciferase units (RLU) was calculated by normalization of luciferase activity to renilla activity. Average RLU was calculated from duplicate samples and standard deviations are shown. B) FGFR2 R1 ES cells containing stably integrated 330bp *Nanog* β-geo reporter were stably transfected with the 330 bp luciferase reporter plasmid or C) FGFR2 R1 ES cells were stably integrated with a 330 bp *Nanog* β-geo plasmid lacking HRPT homologous arms. Cells were harvested after 0 and 6 hours of treatment with AP20187 (10 nM). Real-time PCR was performed to examine expression of *Nanog* and *β-geo* transcripts. mRNA value relative to *β-actin* is expressed as fold change over time, where 0 hrs is set to a value of 1. .

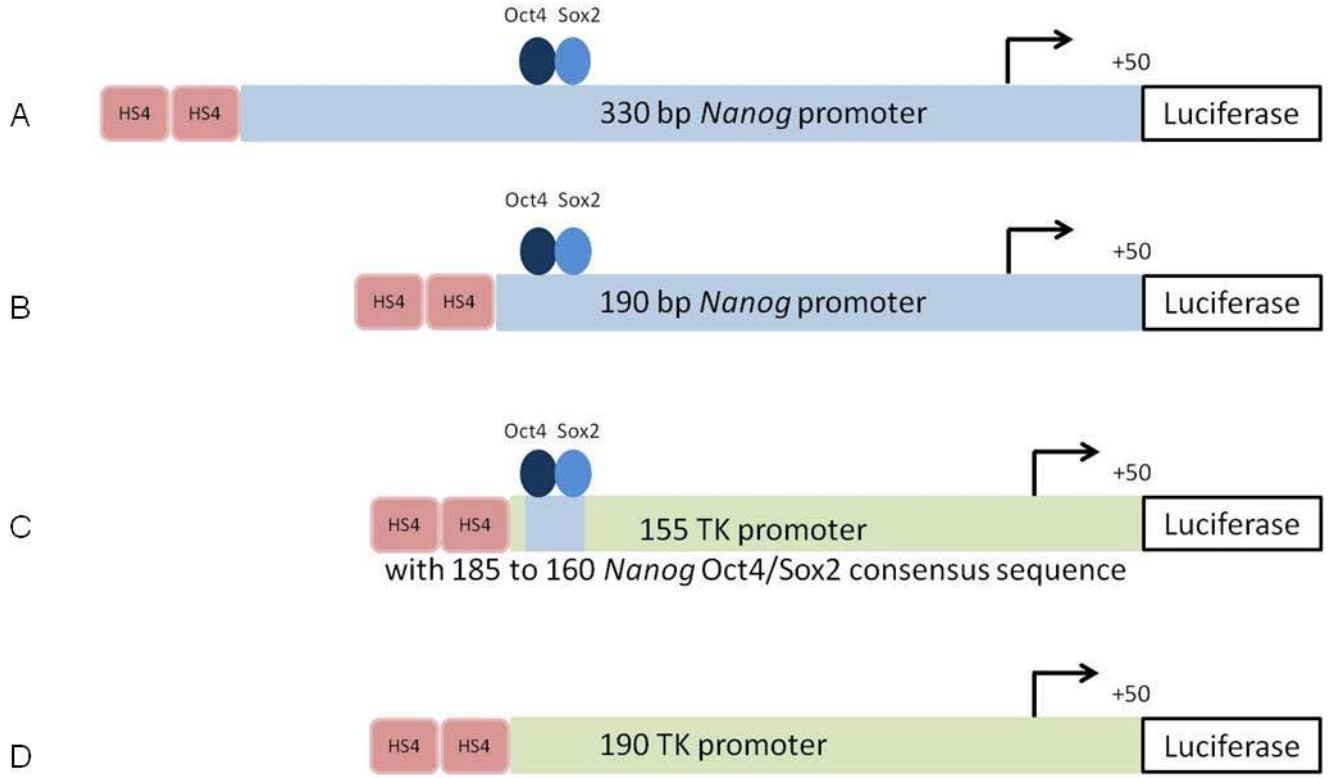

Figure 3-13. Schematic of insulated *Nanog* promoter or TK promoter reporters. Two copies of HS4 insulator elements from the chicken β-globin locus are shown in red and located 5' to the reporter transgene. A) 330 and B) 190 bp *Nanog* promoters contain only *Nanog* promoter sequence driving luciferase reporter activity. C) Oct4/Sox2 consensus sequence from the *Nanog* locus was inserted upstream of the thymidine kinase minimal promoter and D) 190 bp thymidine kinase control reporter lacks endogenous *Nanog* sequence, containing only thymidine kinase promoter driving luciferase reporter activity.

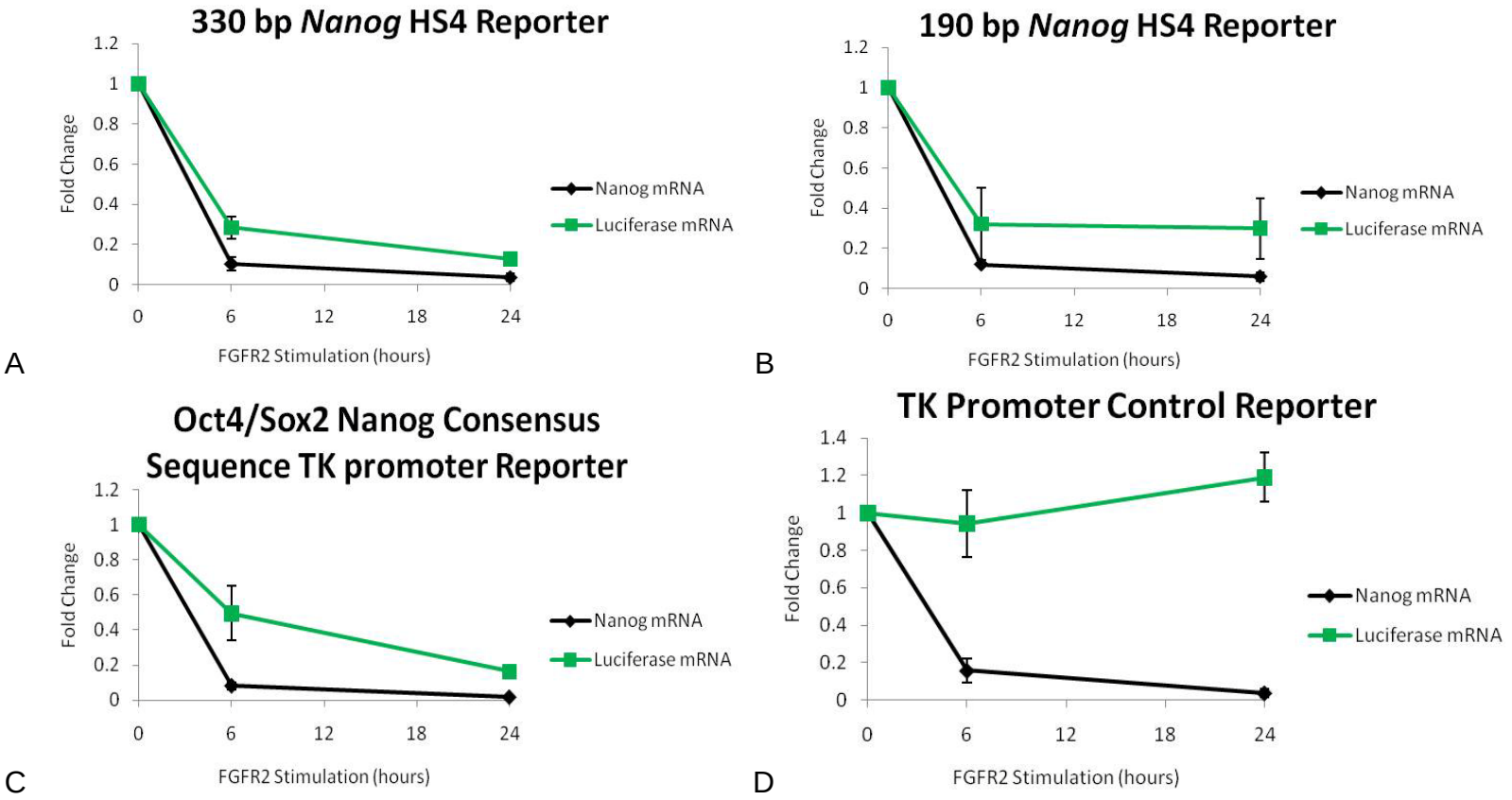

Figure 3-14. The Oct4 and Sox2 consensus binding sites are sufficient for FGFR2 mediated *Nanog* repression. FGFR2 ES cells were stably integrated with A) 330 bp *Nanog* promoter B) 190 bp *Nanog* Promoter, C) Oct4/Sox2 *Nanog* TK promoter, or D) control TK promoter. Insulated *Nanog* reporter cell lines were harvested after 0, 6, or 24 hours of treatment with AP20187 (10 nM). Real-time PCR was performed to examine expression of endogenous *Nanog* or *luciferase* transcripts. Average mRNA expression value relative to *β-actin* is expressed as fold change over time, where 0 hrs is set to a value of 1. Each graph displays average values of four clones, with two experiments for each clone. Error bars indicate standard deviation.

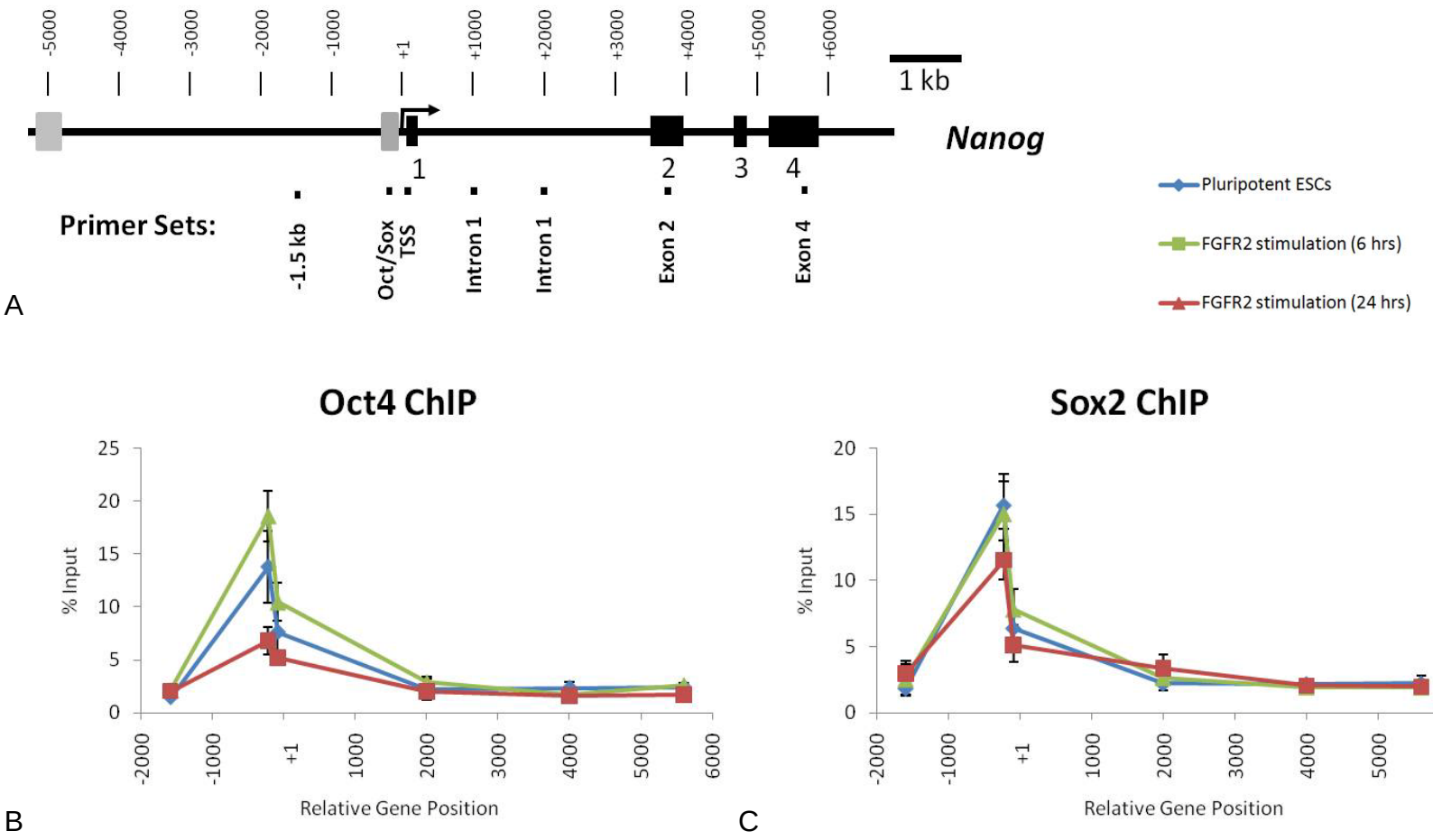

Figure 3-15. FGFR2 homodimerization does not induce Oct4 and Sox2 dissociation from the *Nanog* promoter region. A) Schematic of *Nanog* locus with location of real-time PCR primers for analysis of chromatin immunoprecipitation assays. Real-time PCR analysis of enrichment of A) Oct4 or B) Sox2 at the *Nanog* locus in ES cells harvested after 0, 6, or 24 hours of treatment with AP20187 (10 nM). Enrichment is expressed as % input. Samples were run in triplicate for each primer and the average % input is plotted. Error bars indicate standard deviation.

CHAPTER 4
CONCLUSIONS AND DISCUSSION

One of the earliest cell specification processes during embryonic development involves commitment of pluripotent cells of the inner cell mass to either the epiblast lineage, which forms the embryo proper, or to the extraembryonic primitive endoderm lineage, which sustains the developing embryo. This process begins in the early blastocyst stage embryo when two transcription factors Nanog and Gata6 are heterogeneously expressed and fluctuate in individual cells[59,68]. Strikingly, these fluctuations are resolved and cells are properly sorted by the late blastocyst stage, where inner, epiblast cells express Nanog, and outer primitive endoderm cells express Gata6[16]. While FGFR activation of MAPK signaling has been demonstrated to be central to this process of PE commitment, it is poorly understood how *Nanog* is ultimately downregulated to allow for *Gata6* expression and subsequent specification to PE. Pluripotent ES cells are a powerful experimental model to study these questions, as they are derived from the blastocyst ICM cells, can be cultured indefinitely *in vitro*, and share essential features of ICM cells including heterogeneous and fluctuating Nanog and Gata6 expression, and plasticity in fate specification[58].

The present work has demonstrated a powerful system to induce FGFR2 homodimerization and activate MAPK Mek/Erk signaling to recapitulate PE specification in ES cells. We demonstrate that robust stimulation of ES cells containing an inducible FGFR2 kinase domain using the synthetic chemical dimerizer AP20187 activates MAPK signaling and Erk1/2 phosphorylation, and is able to overcome heterogeneity of Nanog and Gata6 expression to induce *Nanog* downregulation and PE differentiation. Using

inhibitors of FGFR, PI3K, or Mek1/2, we demonstrate the importance of the Mek signal in mediating *Nanog* downregulation. Indeed, FGFR2 dimerization selectively downregulates *Nanog* among the key pluripotency transcription factors Nanog, Oct4, and Sox2.

The reduction in *Nanog* transcripts, which can be seen within 1 hour and reaches over 80% by 6 hours suggests *Nanog* has a short half-life or that transcript is actively degraded upon FGFR2 stimulation. Indeed, *Nanog* is likely transcriptionally downregulated as both pre-spliced and mature mRNA are similarly reduced. In accordance with these results we also found that the histone modification H3K36me3, which is associated with transcriptional elongation, is decreased after FGFR2 stimulation, indicating a reduction in elongating *Nanog* transcripts. Surprisingly, RNA Polymerase II phosphorylated at serine 5 is not rapidly lost following 6 hours of FGFR2 dimerization, but is rather transiently enriched. This phosphorylated form of the enzyme is associated with transcript initiation, and accumulation around the transcription start site at 6 hours at a time when *Nanog* is reduced to over 90% suggests progressive elongation is not occurring. The persistence of RNA polymerase II enrichment could potentially be explained by RNA Polymerase II stalling following initiation in the *Nanog* locus. Further examination of the serine 2 and 5 phosphorylated form of the RNA Polymerase II enzyme associated with transcriptional elongation could provide a more complete picture.

Interestingly, when we examined the histone modification H3K4me3, which is associated with active chromatin, we noticed a change in localization of the modification from the transcription start site localization seen in undifferentiated ES cells, to a more

broad distribution to include enrichment further upstream in the promoter and further downstream into the gene body. The enrichment in components related to active transcription, including RNA Polymerase II and H3K4me3, which were not rapidly lost even when *Nanog* was downregulated may be related to natural fluctuations seen in *Nanog* in ES cell culture[68] and lend support to the idea that cells derived from the ICM are plastic in their expression of Nanog and Gata6[15]. The ability of cells which are not actively expressing *Nanog* to maintain the locus in a poised state may facilitate the rapid re-expression of the gene during the stage when expression of Gata6 and Nanog are fluctuating prior to cell commitment to EPI or PE.

In addition, we have demonstrated that a very minimal promoter region is required for mediating *Nanog* downregulation in response to FGFR2 stimulation. Interestingly, this region is known to bind critical transcriptional activators Oct4 and Sox2[46,47]. We observed *Oct4* and *Sox2* mRNA, protein expression, and binding to the *Nanog* promoter region was also maintained in FGFR2 stimulated cells. When considering a mechanism for *Nanog* repression there are a variety of possibilities including prevention of activator binding, activator degradation, quenching of an activator by a repressor, altering chromatin structure, and inhibition of transcriptional elongation. While it is possible Oct4 and Sox2 do not play a role in *Nanog* repression, the region sufficient for mediating *Nanog* repression is quite short and is largely taken up by the binding of these proteins. Looking at our experimental data of Oct4 and Sox2 persistence following FGFR2 stimulation, it does not appear that simple interference with activator binding or activator degradation is the primary mechanism for *Nanog* repression. A few possibility are that FGFR2 dimerization may induce association of repressor proteins with Oct4 or Sox2 to

mask its activation domain, or Oct4 and Sox2 may serve as a scaffold for factors involved in transcriptional activation of the *Nanog* locus in undifferentiated cells and upon differentiation, these factors are replaced by proteins associated with gene repression. Previously, the co-activator p300 has been shown to associate with Oct4[69] in undifferentiated ES cells. Though we saw a slight enrichment in p300 binding around the *Nanog* transcription start site, this association was not significantly altered in ES cells following FGFR2 dimerization.

Previously, Oct4 and Sox2 have been shown to bind to the promoter of a large number of genes in ES cells, including both active and repressed genes[39,48]. Currently, it is not known how Oct4 and Sox2 binding can result in both activation and repression of these genes. Several genes which are known to be positively regulated by Oct4 and Sox2 in ES cells include *Nanog*, *Fgf4*, *Oct4*, *Sox2*, *Utf1*, *Fbx15*, and *Lefty1*. Using real-time PCR we have found that FGFR2 dimerization results in downregulation of *Nanog* and *Fgf4*, but not the other genes in this list. We hypothesize the specificity of downregulation of these genes is due to Oct4/Sox2 binding sequence and local chromatin organization. Construction of reporters replacing the *Nanog* Oct4/Sox2 binding sequence with that of the responsive gene *Fgf4* or the unresponsive genes, including *Utf1*, will lead to greater understanding of the repression mechanism. The present study provides an insight for molecular mechanisms underlying how FGFR2 dominates early cell fate decision between epiblast and hypoblast in a potentially reversible manner. The FGFR2 dimerization system developed here would be useful for further dissecting effectors of *Nanog* downregulation.

Nanog de-repression is also an important issue in the context of induced pluripotent stem cell (iPSC) generation, which is a recently discovered method to reprogram somatic cells to a pluripotent state[69,70]. The classical factors used to accomplish this were Oct4, Sox2, Klf4, and c-Myc, where Klf4 and c-Myc are thought to induce profound chromatin changes, while Oct4 and Sox2 are important for re-expression of critical pluripotency genes including *Nanog*. While exogenous *Nanog* expression is not required for iPSC generation, it has been demonstrated that Nanog, Oct4, Sox2, and Lin28 are also able to reprogram somatic cells[71]. Notably, use of a Mekinhibitor has also been shown to increase iPSC generation efficiency[72]. Since FGF is included in serum used in culture media, prevention of *Nanog* downregulation through the Mek inhibitor likely plays a critical role. Interestingly, there is evidence that *Nanog* is re-expressed in certain tumors including germ cell tumors[73], and in a subset of cancer cells which display stem-cell like characteristics[74], indicating that understanding *Nanog* repression could lead to improved cancer therapeutics. In conclusion, a thorough understanding of *Nanog* regulation may impact areas beyond the context of developmental biology.

LIST OF REFERENCES

1. Ahmed K, Dehghani H, Rugg-Gunn P, et al. Global chromatin architecture reflects pluripotency and lineage commitment in the early mouse embryo. PLoS One. 2010;5:e10531.

2. Cockburn K, Rossant J. Making the blastocyst: lessons from the mouse. J Clin Invest. 2010;120:995-1003.

3. Nagy A, Gertsenstein M, Vintersten K, et al., eds. Manipulating the Mouse Embryo. Third ed. Cold Springs Harbor: Cold Springs Harbor Laboratory Press; 2003.

4. Watson AJ, Barcroft LC. Regulation of blastocyst formation. Front Biosci. 2001;6:D708-730.

5. Tarkowski AK, Wróblewska J. Development of blastomeres of mouse eggs isolated at the 4- and 8-cell stage. J Embryol Exp Morphol. 1967;18:155-180.

6. Johnson MH, Ziomek CA. The foundation of two distinct cell lineages within the mouse morula. Cell. 1981;24:71-80.

7. Yamanaka Y, Ralston A, Stephenson RO, et al. Cell and molecular regulation of the mouse blastocyst. Dev Dyn. 2006;235:2301-2314.

8. Ralston A, Rossant J. Cdx2 acts downstream of cell polarization to cell-autonomously promote trophectoderm fate in the early mouse embryo. Dev Biol. 2008;313:614-629.

9. Palmieri SL, Peter W, Hess H, et al. Oct-4 transcription factor is differentially expressed in the mouse embryo during establishment of the first two extraembryonic cell lineages involved in implantation. Dev Biol. 1994;166:259-267.

10. Pesce M, Schöler HR. Oct-4: control of totipotency and germline determination. Mol Reprod Dev. 2000;55:452-457.

11. Strumpf D, Mao CA, Yamanaka Y, et al. Cdx2 is required for correct cell fate specification and differentiation of trophectoderm in the mouse blastocyst. Development. 2005;132:2093-2102.

12. Nichols J, Zevnik B, Anastassiadis K, et al. Formation of pluripotent stem cells in the mammalian embryo depends on the POU transcription factor Oct4. Cell. 1998;95:379-391.

13. Bielinska M, Narita N, Wilson DB. Distinct roles for visceral endoderm during embryonic mouse development. Int J Dev Biol. 1999;43:183-205.

14. Chambers I, Colby D, Robertson M, et al. Functional expression cloning of Nanog, a pluripotency sustaining factor in embryonic stem cells. Cell. 2003;113:643-655.

15. Mitsui K, Tokuzawa Y, Itoh H, et al. The homeoprotein Nanog is required for maintenance of pluripotency in mouse epiblast and ES cells. Cell. 2003;113:631-642.

16. Chazaud C, Yamanaka Y, Pawson T, et al. Early lineage segregation between epiblast and primitive endoderm in mouse blastocysts through the Grb2-MAPK pathway. Dev Cell. 2006;10:615-624.

17. Thisse B, Thisse C. Functions and regulations of fibroblast growth factor signaling during embryonic development. Dev Biol. 2005;287:390-402.

18. Roux PP, Blenis J. ERK and p38 MAPK-activated protein kinases: a family of protein kinases with diverse biological functions. Microbiol Mol Biol Rev. 2004;68:320-344.

19. Lanner F, Rossant J. The role of FGF/Erk signaling in pluripotent cells. Development. 2010;137:3351-3360.

20. Arman E, Haffner-Krausz R, Chen Y, et al. Targeted disruption of fibroblast growth factor (FGF) receptor 2 suggests a role for FGF signaling in pregastrulation mammalian development. Proc Natl Acad Sci U S A. 1998;95:5082-5087.

21. Chen Y, Li X, Eswarakumar VP, et al. Fibroblast growth factor (FGF) signaling through PI 3-kinase and Akt/PKB is required for embryoid body differentiation. Oncogene. 2000;19:3750-3756.

22. Li L, Arman E, Ekblom P, et al. Distinct GATA6- and laminin-dependent mechanisms regulate endodermal and ectodermal embryonic stem cell fates. Development. 2004;131:5277-5286.

23. Li X, Chen Y, Schéele S, et al. Fibroblast growth factor signaling and basement membrane assembly are connected during epithelial morphogenesis of the embryoid body. J Cell Biol. 2001;153:811-822.

24. Cheng AM, Saxton TM, Sakai R, et al. Mammalian Grb2 regulates multiple steps in embryonic development and malignant transformation. Cell. 1998;95:793-803.

25. Yoshida-Koide U, Matsuda T, Saikawa K, et al. Involvement of Ras in extraembryonic endoderm differentiation of embryonic stem cells. Biochem Biophys Res Commun. 2004;313:475-481.

26. Evans MJ, Kaufman MH. Establishment in culture of pluripotential cells from mouse embryos. Nature. 1981;292:154-156.

27. Martin GR. Isolation of a pluripotent cell line from early mouse embryos cultured in medium conditioned by teratocarcinoma stem cells. Proc Natl Acad Sci U S A. 1981;78:7634-7638.

28. Ralston A, Rossant J. Genetic regulation of stem cell origins in the mouse embryo. Clin Genet. 2005;68:106-112.

29. Niwa H. How is pluripotency determined and maintained? Development. 2007;134:635-646.

30. Williams RL, Hilton DJ, Pease S, et al. Myeloid leukaemia inhibitory factor maintains the developmental potential of embryonic stem cells. Nature. 1988;336:684-687.

31. Smith AG, Heath JK, Donaldson DD, et al. Inhibition of pluripotential embryonic stem cell differentiation by purified polypeptides. Nature. 1988;336:688-690.

32. Niwa H, Burdon T, Chambers I, et al. Self-renewal of pluripotent embryonic stem cells is mediated via activation of STAT3. Genes Dev. 1998;12:2048-2060.

33. Matsuda T, Nakamura T, Nakao K, et al. STAT3 activation is sufficient to maintain an undifferentiated state of mouse embryonic stem cells. EMBO J. 1999;18:4261-4269.

34. Wilson SI, Edlund T. Neural induction: toward a unifying mechanism. Nat Neurosci. 2001;4 Suppl:1161-1168.

35. Zhang J, Li L. BMP signaling and stem cell regulation. Dev Biol. 2005;284:1-11.

36. Ohtsuka S, Dalton S. Molecular and biological properties of pluripotent embryonic stem cells. Gene Ther. 2008;15:74-81.

37. Liu N, Lu M, Tian X, et al. Molecular mechanisms involved in self-renewal and pluripotency of embryonic stem cells. J Cell Physiol. 2007;211:279-286.

38. Ying QL, Nichols J, Chambers I, et al. BMP induction of Id proteins suppresses differentiation and sustains embryonic stem cell self-renewal in collaboration with STAT3. Cell. 2003;115:281-292.

39. Boyer LA, Lee TI, Cole MF, et al. Core transcriptional regulatory circuitry in human embryonic stem cells. Cell. 2005;122:947-956.

40. Yuan H, Corbi N, Basilico C, et al. Developmental-specific activity of the FGF-4 enhancer requires the synergistic action of Sox2 and Oct-3. Genes Dev. 1995;9:2635-2645.

41. Nishimoto M, Fukushima A, Okuda A, et al. The gene for the embryonic stem cell coactivator UTF1 carries a regulatory element which selectively interacts with a complex composed of Oct-3/4 and Sox-2. Mol Cell Biol. 1999;19:5453-5465.

42. Tokuzawa Y, Kaiho E, Maruyama M, et al. Fbx15 is a novel target of Oct3/4 but is dispensable for embryonic stem cell self-renewal and mouse development. Mol Cell Biol. 2003;23:2699-2708.

43. Nakatake Y, Fukui N, Iwamatsu Y, et al. Klf4 cooperates with Oct3/4 and Sox2 to activate the Lefty1 core promoter in embryonic stem cells. Mol Cell Biol. 2006;26:7772-7782.

44. Okumura-Nakanishi S, Saito M, Niwa H, et al. Oct-3/4 and Sox2 regulate Oct-3/4 gene in embryonic stem cells. J Biol Chem. 2005;280:5307-5317.

45. Tomioka M, Nishimoto M, Miyagi S, et al. Identification of Sox-2 regulatory region which is under the control of Oct-3/4-Sox-2 complex. Nucleic Acids Res. 2002;30:3202-3213.

46. Rodda DJ, Chew JL, Lim LH, et al. Transcriptional regulation of nanog by OCT4 and SOX2. J Biol Chem. 2005;280:24731-24737.

47. Kuroda T, Tada M, Kubota H, et al. Octamer and Sox elements are required for transcriptional cis regulation of Nanog gene expression. Mol Cell Biol. 2005;25:2475-2485.

48. Loh YH, Wu Q, Chew JL, et al. The Oct4 and Nanog transcription network regulates pluripotency in mouse embryonic stem cells. Nat Genet. 2006;38:431-440.

49. Doetschman TC, Eistetter H, Katz M, et al. The in vitro development of blastocyst-derived embryonic stem cell lines: formation of visceral yolk sac, blood islands and myocardium. J Embryol Exp Morphol. 1985;87:27-45.

50. Hamazaki T, Oka M, Yamanaka S, et al. Aggregation of embryonic stem cells induces Nanog repression and primitive endoderm differentiation. J Cell Sci. 2004;117:5681-5686.

51. Hamazaki T, Kehoe SM, Nakano T, et al. The Grb2/Mek pathway represses Nanog in murine embryonic stem cells. Mol Cell Biol. 2006;26:7539-7549.

52. Pan G, Li J, Zhou Y, et al. A negative feedback loop of transcription factors that controls stem cell pluripotency and self-renewal. FASEB J. 2006;20:1730-1732.

53. Chen X, Fang F, Liou YC, et al. Zfp143 regulates Nanog through modulation of Oct4 binding. Stem Cells. 2008;26:2759-2767.

54. Suzuki A, Raya A, Kawakami Y, et al. Nanog binds to Smad1 and blocks bone morphogenetic protein-induced differentiation of embryonic stem cells. Proc Natl Acad Sci U S A. 2006;103:10294-10299.

55. Jiang J, Chan YS, Loh YH, et al. A core Klf circuitry regulates self-renewal of embryonic stem cells. Nat Cell Biol. 2008;10:353-360.

56. Wu Q, Chen X, Zhang J, et al. Sall4 interacts with Nanog and co-occupies Nanog genomic sites in embryonic stem cells. J Biol Chem. 2006;281:24090-24094.

57. Pereira L, Yi F, Merrill BJ. Repression of Nanog gene transcription by Tcf3 limits embryonic stem cell self-renewal. Mol Cell Biol. 2006;26:7479-7491.

58. Gu P, LeMenuet D, Chung AC, et al. Orphan nuclear receptor GCNF is required for the repression of pluripotency genes during retinoic acid-induced embryonic stem cell differentiation. Mol Cell Biol. 2005;25:8507-8519.

59. Lin T, Chao C, Saito S, et al. p53 induces differentiation of mouse embryonic stem cells by suppressing Nanog expression. Nat Cell Biol. 2005;7:165-171.

60. Singh AM, Hamazaki T, Hankowski KE, et al. A heterogeneous expression pattern for Nanog in embryonic stem cells. Stem Cells. 2007;25:2534-2542.

61. Steve R, Skaletsky H. Primer3 on the WWW for general users and for biologist programmers. In: Krawetz S, Misener S, eds. Bioinformatics Methods and Protocols: Methods in Molecular Biology. Totowa, NJ: Humana Press; 2000:365-386.

62. Alfa RW, Tuszynski MH, Blesch A. A novel inducible tyrosine kinase receptor to regulate signal transduction and neurite outgrowth. J Neurosci Res. 2009;87:2624-2631.

63. Xian W, Pappas L, Pandya D, et al. Fibroblast growth factor receptor 1-transformed mammary epithelial cells are dependent on RSK activity for growth and survival. Cancer Res. 2009;69:2244-2251.

64. Kwiatkowski BA, Kirillova I, Richard RE, et al. FGFR4 and its novel splice form in myogenic cells: Interplay of glycosylation and tyrosine phosphorylation. J Cell Physiol. 2008;215:803-817.

65. Ying QL, Wray J, Nichols J, et al. The ground state of embryonic stem cell self-renewal. Nature. 2008;453:519-523.

66. Edmunds JW, Mahadevan LC, Clayton AL. Dynamic histone H3 methylation during gene induction: HYPB/Setd2 mediates all H3K36 trimethylation. EMBO J. 2008;27:406-420.

67. Li B, Carey M, Workman JL. The role of chromatin during transcription. Cell. 2007;128:707-719.

68. Chambers I, Silva J, Colby D, et al. Nanog safeguards pluripotency and mediates germline development. Nature. 2007;450:1230-1234.

69. Chen X, Xu H, Yuan P, et al. Integration of external signaling pathways with the core transcriptional network in embryonic stem cells. Cell. 2008;133:1106-1117.

70 Takahashi K, Tanabe K, Ohnuki M, et al. Induction of pluripotent stem cells from adult human fibroblasts by defined factors. Cell. 2007; 131:861-872.

71. Yu J, Vodyanik MA, Smuga-Otto K, et al. Induced pluripotent stem cell lines derived from human somatic cells. Science. 2007;318:1917-1920.

72 Lin T, Ambasudhan R, Yuan X, et al. A chemical platform for improved induction of human iPSCs. Nat Methods. 2009; 6:805-808.

73. Hart AH, Hartley L, Parker K, et al. The pluripotency homeobox gene NANOG is expressed in human germ cell tumors. Cancer. 2005;104:2092-2098.

74. Levings PP, McGarry SV, Currie TP, et al. Expression of an exogenous human Oct-4 promoter identifies tumor-initiating cells in osteosarcoma. Cancer Res. 2009;69:5648-5655.

BIOGRAPHICAL SKETCH

Katherine Elizabeth Hankowski was born in Springfield, Massachusetts in 1982 to Marguerite and Alan. She grew up in the nearby towns of Amherst and Northampton, Massachusetts with her older brother Alex and younger sister Christina. After graduating from Deerfield Academy in 2001, she attended Hamilton College in Clinton, New York for undergraduate studies. She received her Bachelor of Arts degree in neuroscience in 2005. In the fall of 2005, she began her graduate studies in the Interdisciplinary Program for Biomedical Research at the University of Florida with a concentration in molecular cell biology. She joined the laboratory of Naohiro Terada, M.D., Ph.D. in the summer of 2006.